AD-A111 649 UNITED TECHNOLOGIES RESEARCH CENTER EAST HARTFORD CT F/G 13/8
FABRICATION OF THIN WALL CYLINDRICAL SHELLS BY SPUTTERING.(U)
NOV 81 E L PARADIS N00019-78-C-0502
UNCLASSIFIED UTRC/R80-924394-8 NL

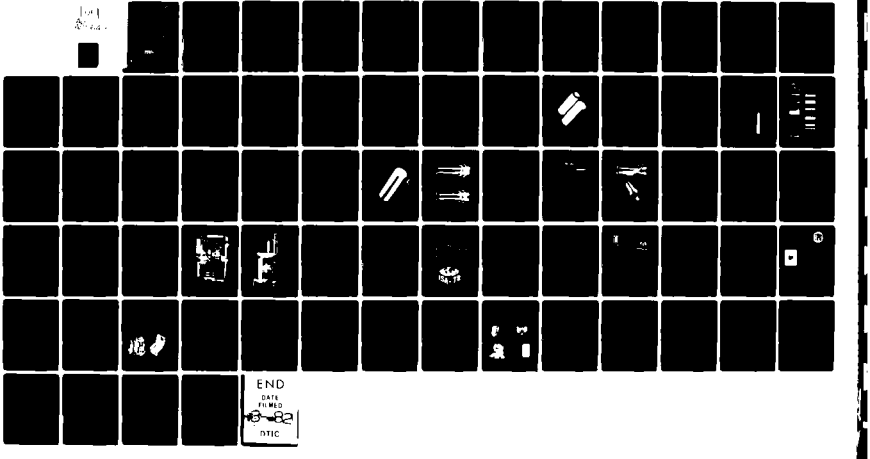

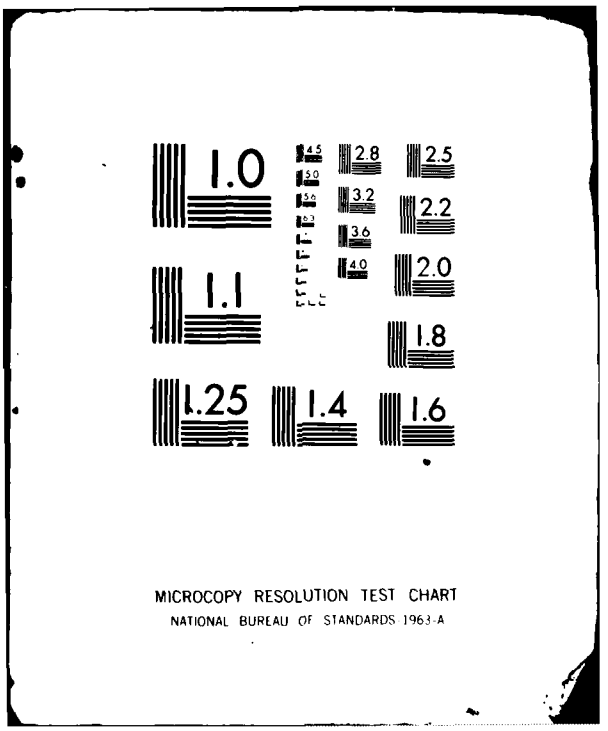
1.0
1.1
1.25
1.4
1.6
1.8
2.0
2.2
2.5
2.8
3.2
3.6
4.0
4.5
5.0
MICROCOPY RESOLUTION TEST CHART
NATIONAL BUREAU OF STANDARDS 1963-A

R80-924394-8

12

Fabrication of Thin Wall Cylindrical Shells By Sputtering

Final Technical Report

E.L. Paradis

Prepared under contract N00019-78-C-0502

November 30, 1981

UNITED TECHNOLOGIES RESEARCH CENTER
East Hartford, Connecticut 06108

R80-924394-8

Fabrication of Thin Wall Cylindrical Shells by Sputtering

Final Technical Report

E. L. Paradis

United Technologies Research Center
East Hartford, Connecticut 06108

Prepared Under Contract N00019-78-C-0502

November 30, 1981

UNCLASSIFIED

SECURITY CLASSIFICATION OF THIS PAGE (When Data Entered)

REPORT DOCUMENTATION PAGE		READ INSTRUCTIONS BEFORE COMPLETING FORM
1. REPORT NUMBER	2. GOVT ACCESSION NO.	3. RECIPIENT'S CATALOG NUMBER
4. TITLE (and Subtitle) Fabrication of Thin Wall Cylindrical Shells by Sputtering		5. TYPE OF REPORT & PERIOD COVERED Final Technical Report 4 Aug. '78 to 4 Aug. '80
		6. PERFORMING ORG. REPORT NUMBER R80-924394-8
7. AUTHOR(s) E. L. Paradis		8. CONTRACT OR GRANT NUMBER(s) N00019-78-C-0502
9. PERFORMING ORGANIZATION NAME AND ADDRESS United Technologies Research Center Silver Lane East Hartford, Connecticut 06108		10. PROGRAM ELEMENT, PROJECT, TASK AREA & WORK UNIT NUMBERS
11. CONTROLLING OFFICE NAME AND ADDRESS Naval Air Systems Command Washington, D. C. 20361 Contract Monitor: Steven Linder AIR 5162C		12. REPORT DATE 30 Nov. 1981 13. NUMBER OF PAGES
14. MONITORING AGENCY NAME & ADDRESS(if different from Controlling Office)		15. SECURITY CLASS. (of this report) Unclassified 15a. DECLASSIFICATION/DOWNGRADING SCHEDULE

16. DISTRIBUTION STATEMENT (of this Report)

Approved for Public Release, Distribution Unlimited

17. DISTRIBUTION STATEMENT (of the abstract entered in Block 20, if different from Report)

18. SUPPLEMENTARY NOTES

19. KEY WORDS (Continue on reverse side if necessary and identify by block number)

Thin Wall Cylinders
Pressure Transducers
Vibrating Cylinders
Sputtering
Free Standing Films

20. ABSTRACT (Continue on reverse side if necessary and identify by block number)

This report describes the process used to fabricate thin wall cylindrical shells by sputtering. The shells are grown on both sacrificial aluminum and reuseable stainless steel mandrels. The post deposition process used to remove the shells from the mandrels is described. The effect of deposition conditions and post deposition treatment on crystallographic structure is presented. Comparisons of sputtered shells are made with conventionally ...

DD FORM 1 JAN 73 1473 EDITION OF 1 NOV 65 IS OBSOLETE
S/N 0102-LF-014-6601

UNCLASSIFIED

SECURITY CLASSIFICATION OF THIS PAGE (When Data Entered)

machined ones as pertains to dimensional uniformity and performance. Test results of sputtered thin wall cylindrical shells used as pressure sensing elements are given.

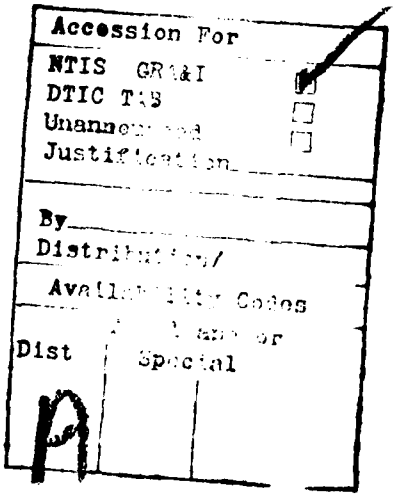

Fabrication of Thin Wall Cylindrical Shells by Sputtering

TABLE OF CONTENTS

LIST OF FIGURES

LIST OF FIGURES (Cont'd)

LIST OF TABLES

FOREWORD

Publication of this report does not constitute approval by the Naval Air Systems Command of the findings or conclusions contained herein. It is published for the exchange and stimulation of ideas.

ACKNOWLEDGMENTS

The author is pleased to acknowledge the important contributions to this program made by the following members of the UTRC staff: to D. H. Grantham for Program Management, to G. Drake for experimental measurements and especially to D. G. Mankee who set up and operated the sputtering systems which produced the thin wall shells. The author also wishes to thank M. Latina of United Technologies Hamilton Standard Division for all of his help and valuable comments throughout this program.

R80-924394-8

Fabrication of Thin Wall Cylindrical Shells by Sputtering

SUMMARY

Work under this program was directed toward establishing a low cost method of fabricating thin walled cylindrical shells using the sputtering process. These thin wall shells were to be used as the sensing element in a thin wall vibrating cylinder pressure transducer.

The goals of the program were to complete a Manufacturing Technology Program to establish the sputtering process parameters and associated technology required to:

1) produce by sputtering thin walled cylindrical shells whose mechanical and magnetic properties were such as to operate as the sensing elements in vibrating cylinder pressure transducers,

2) demonstrate that the use of the sputtering process for fabricating the cylindrical shells was cost effective as compared with the present practice of machining.

Currently, the thin wall cylinders used in the Vibrasense® pressure transducer manufactured by Hamilton Standard Division of United Technologies are fabricated from bulk material using conventional machining techniques. In this program, we have been able to develop a technique to fabricate thin wall shells by sputtering. Wall thickness and thickness uniformity specifications have been able to be maintained using this technology. The sputtered cylinder can be made vacuum tight as required for use in the vibrating cylinder pressure transducer. Also, the sputtered shells have the necessary magnetic properties to be able to be driven by the electromagnetic driving field. However, the crystallographic properties of the sputtered shells have not been able to be made to match those of the bulk material. As a result, the sputtered shells have not been able to achieve the sharp resonance attained by the machined shells. This has manifested itself as a low quality (Q) factor in testing and low signal output.

The cylinders are made of Ni-Span-C_1 Alloy 902. This is a very complex 10 component alloy with some reactive components such as titanium, aluminum and iron. While the compositional ratios of the components has been maintained during the sputtering process, the grain growth in the sputtered film has resulted in yielding inferior mechanical properties to that of the bulk. Post deposition treatments

which included cold working and heat treatment did not appear to improve the mechanical properties or change the crystallographic morphology. It is felt that the highly reactive metal components of the alloy combined readily with any contaminants of the system and form compounds which acted as pinning sites to inhibit grain growth even during heat treatment.

It is felt at this time that the technology should be pursued in order to achieve the high mechanical performance required in the thin wall cylinder application. A further program is suggested using less complex alloys, and even a pure metal, to determine the deposition conditions required to achieve bulk mechanical properties which it is felt could still be attained with this technology. With the proper deposition parameters thus in control, bulk quality Ni-Span-C could be deposited.

In accordance with the requirement of the contract, two thin wall cylinders of the type used in the Hamilton Standard Vibrasense^{R} were delivered to the Naval Air Systems Command as well as a demonstration Vibrasense^{R} unit utilizing a sputtered thin wall cylinder as the sensor unit.

A total of 110 runs were made in this program in order to establish the proper deposition parameters. The parameters investigated were: sputtering gas - pressure and type, deposition rate, substrate temperature, substrate bias and magnetic field strength.

1. INTRODUCTION

The vibrating cylinder pressure transducer is a unique device which measures pressures to state-of-the-art accuracies. The transducer provides a frequency output proportional to pressure which is ideally suited for digital interface. The sensing element consists of an assembly of two concentric closed-end cylinders -- a vibrating inner one and a protective outer one. These cylinders are fastened to a common base at one end and are free at the other. A schematic representation of this configuration is shown in Fig. 1. An additional central structure is built from the base, and this is called the spool body. The spool body serves as a support for electromagnets used in (1) exciting or driving the vibrating inner cylinder, and (2) detecting its motion and frequency. The space between the vibrating inner cylinder and the protective outer cylinder is evacuated to serve as the absolute pressure reference. The cavity volume between the vibrating inner cylinder and the spool body receives the input pressure, generally through porting passages in the transducer base.

The side wall of the inner cylinder is excited by magnetic field forces generated with the electromagnetic driver coil located on the spool body. The inner cylinder vibrates at its lowest natural frequency relative to its physical dimensions, which also corresponds to its lowest energy level. Figure 2 illustrates the fundamental and higher order modes at which a cylinder may vibrate. The modes that are utilized in the Vibrasense^{R} are the $n = 4$; $m = 1$.

A pneumatic pressure can be introduced into the cavity between the spool body and the vibrating cylinder. The wall elements of the cylinder are tensioned by the pressure acting over the cylinder internal area, and this tension causes the cylinder natural frequency to increase as a function of the increased pressure. When the mechanical frequency increases, the magnetic pickup coil immediately detects this and instantaneously relays this information to the amplifier-limiter combination. This new frequency and a new limiting voltage are fed back to the driver coil to produce a reinforcing force pulse at the proper frequency.

Such a transducer is currently being manufactured by Hamilton Standard Division of United Technologies Corporation. An article more fully describing its operation and capabilities is reproduced in Appendix I. The cylindrical shells are currently made by machining from a tube of Ni-Span-C metal alloy. However, because of this method of fabrication, not only are the cylinders very expensive, because of the precision of the machining required, but sizes and wall thicknesses are limited to what can be accurately machined. Another cylinder fabrication method being investigated by Hamilton Standard is that of electroforming the cylinder on a sacrificial mandrel. Results to date have not been encouraging because this method is limited to materials which can be electroplated. Ni-Span-C, for example, cannot be electroplated because of the presence of titanium in its composition. However, Ni-Span-C

FIG. 1

CONSTRUCTION AND OPERATING PRINCIPLE OF VIBRATING CYLINDER PRESSURE TRANSDUCER

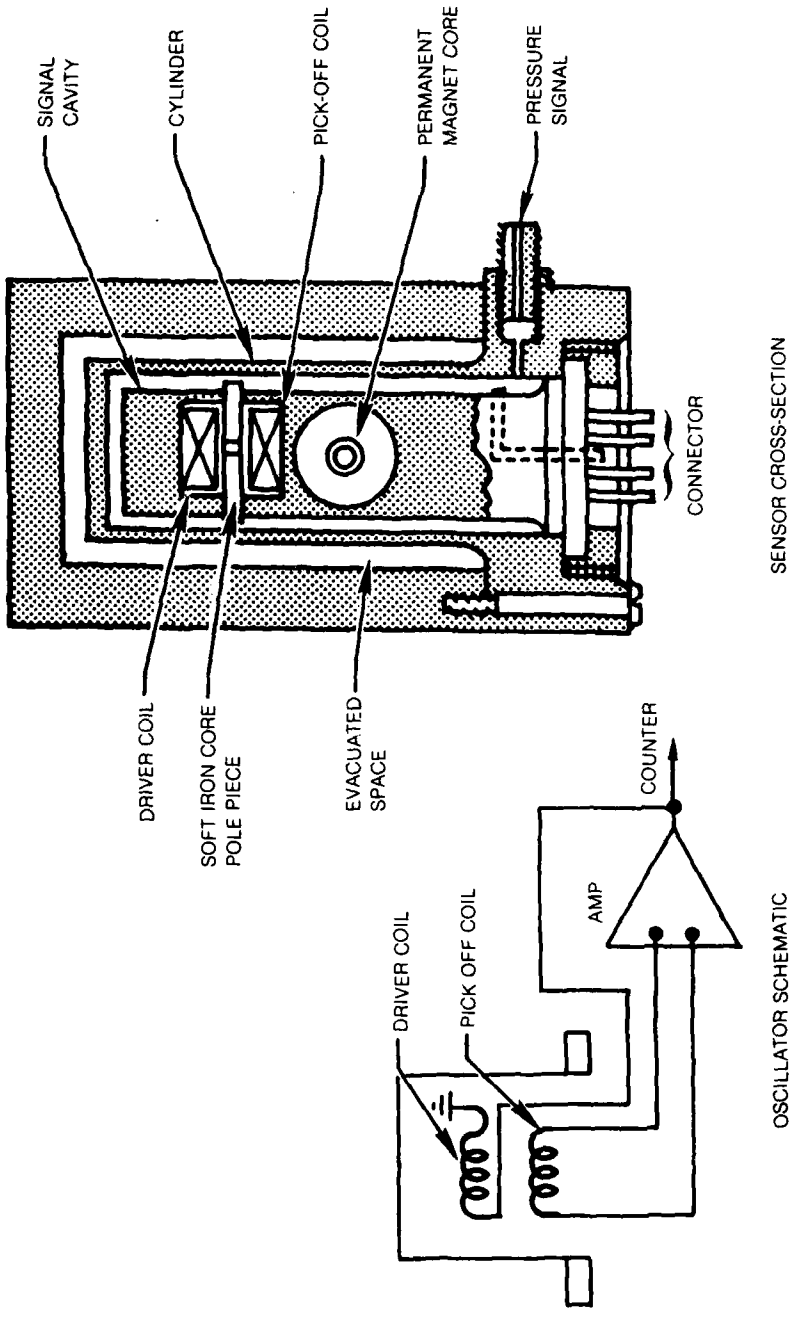

80-8-3-8

SOME MODES OF VIBRATION OF A CYLINDER

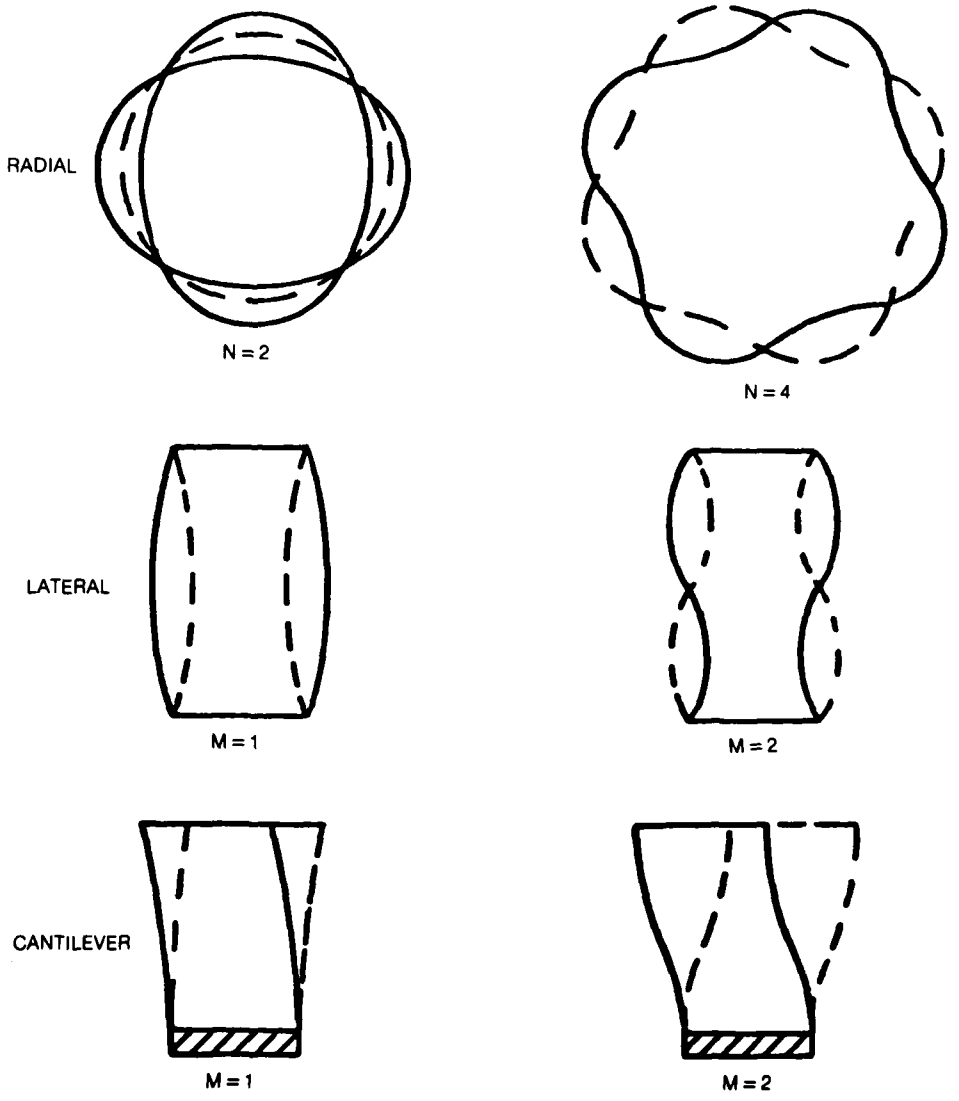

80-8-3-9

remains an attractive materials for this application because its acoustic modulus varies slowly with temperature, a property which contributes greatly to its operating stability.

Ni-Span-C also has a reasonably high yield point so that the normal working stress is only a small percent of its yield strength. This results in negligible stress creep - an important factor in maintaining long term stability. Ni-Span-C has a long history of use in mechanical resonators, Bourdon tubes, aneroid capsules, etc.

The sputtering process has the ability of depositing complex alloys while maintaining the composition of the bulk. Therefore, alloys such as Ni-Span-C could be deposited by sputtering. Furthermore, Hamilton Standard has found that one of the problems encountered in the fabrication of the present thin walled shells is the inconsistency in the properties of the Ni-Span-C stock. As a result, considerable variations exist in the behavior of the shells and adjustments in the electronics must be made to compensate. In sputtering, very little material is wasted as compared to conventional machining processes. Therefore, one sputtering target could be used to fabricate many thin wall cylindrical shells with essentially identical physical and magnetic properties.

Once the sputtering technique has been established, thin walled cylinder fabrication cost could be substantially reduced over the current method of machining because sputtering is amenable to batch processing with one operator capable of operating several systems.

The objective of this Manufacturing Technology Program was to establish the sputtering process as a practical method of forming thin wall cylindrical shells for use as the sensing element in vibrating cylinder pressure transducers of the type currently used in jet engine aircraft. In order to reach this objective, the goals of the program were:

1. To determine the sputtering process parameters and to develop the associated technology required to produce by sputtering thin wall cylindrical shells whose mechanical and magnetic properties are such as to operate as the sening element in vibrating cylinder pressure transducers.

2. To demonstrate that the use of the sputtering process for fabricating the cylindrical shells is cost effective as compared to the present method of machining.

Since the nickel alloy Ni-Span-C has been used to fabricate the thin wall cylinders used in the Vibrasense^{R}, and since a great deal is known by Hamilton Standard about its operating characteristics as a vibrating cylinder pressure transducer, this material was chosen for use in this program so that progress could be established relative to a known standard.

2. DETAILS OF FABRICATION

The basic approach used in this program to fabricate the thin wall shells was to deposit Ni-Span-C by sputtering onto a rotating mandrel. After the desired thickness of Ni-Span-C had been deposited, the sputtered shell had to be removed from the mandrel. To accomplish this, the major technical problems to be solved were:

1. Deposit the Ni-Span-C such that it had the required mechanical and magnetic properties necessary for use as a vibrating cylinder pressure transducer, and

2. Find a suitable means of removing the thin wall shell from the mandrel.

2.1 Sputtering Facilities

The sputtering facility in which the greater part of the work of this contract was carried on was an 18 inch high by 18 inch diameter stainless steel vacuum chamber pumped with a 1600 liter per second turbomolecular pump back by a mechanical roughing pump. The cylindrical shells were formed by depositing onto a rotating mandrel from one or two planar 5 inch diameter rf diode sputtering targets. In some instances a third target was used. The third target was mounted so that it was oriented 90 degrees to the two opposed targets and in line with the mandrel. The third target was used to build up surfaces on the cylinder which were perpendicular to the cylindrical axis. The shaft which supported the mandrel was hollow to accommodate a heater and a temperature sensor. Furthermore, an electrical bias could be applied to the mandrel through the rotating shaft. The mandrel was threaded internally and screwed onto the rotatable shaft. A pair of electromagnets behind and concentric with the targets was used to support and confine the plasma in the vicinity of the target. A schematic diagram of this sputtering facility is shown in Fig. 3.

A second sputtering facility was used for a portion of this work when operation and reliability of the primary system became suspect. The vacuum chamber was also of stainless steel but in the shape of a six sided cross. The cross was fabricated from 6.25 inch diameter pipe. The chamber was pumped with a six inch diameter oil diffusion pump and a mechanical backing pump. The internal fixturing for the targets and substrate was similar to the first system described except that it was rotated 90 degrees with the targets sputtering in the horizontal direction instead of vertical. In this configuration, it was felt the likelihood of flakes falling on the substrate during deposition would be greatly reduced. A schematic diagram of this sputtering system is shown in Fig. 4.

FIG. 3

PLANAR OPPOSED TARGET SPUTTERING SYSTEM

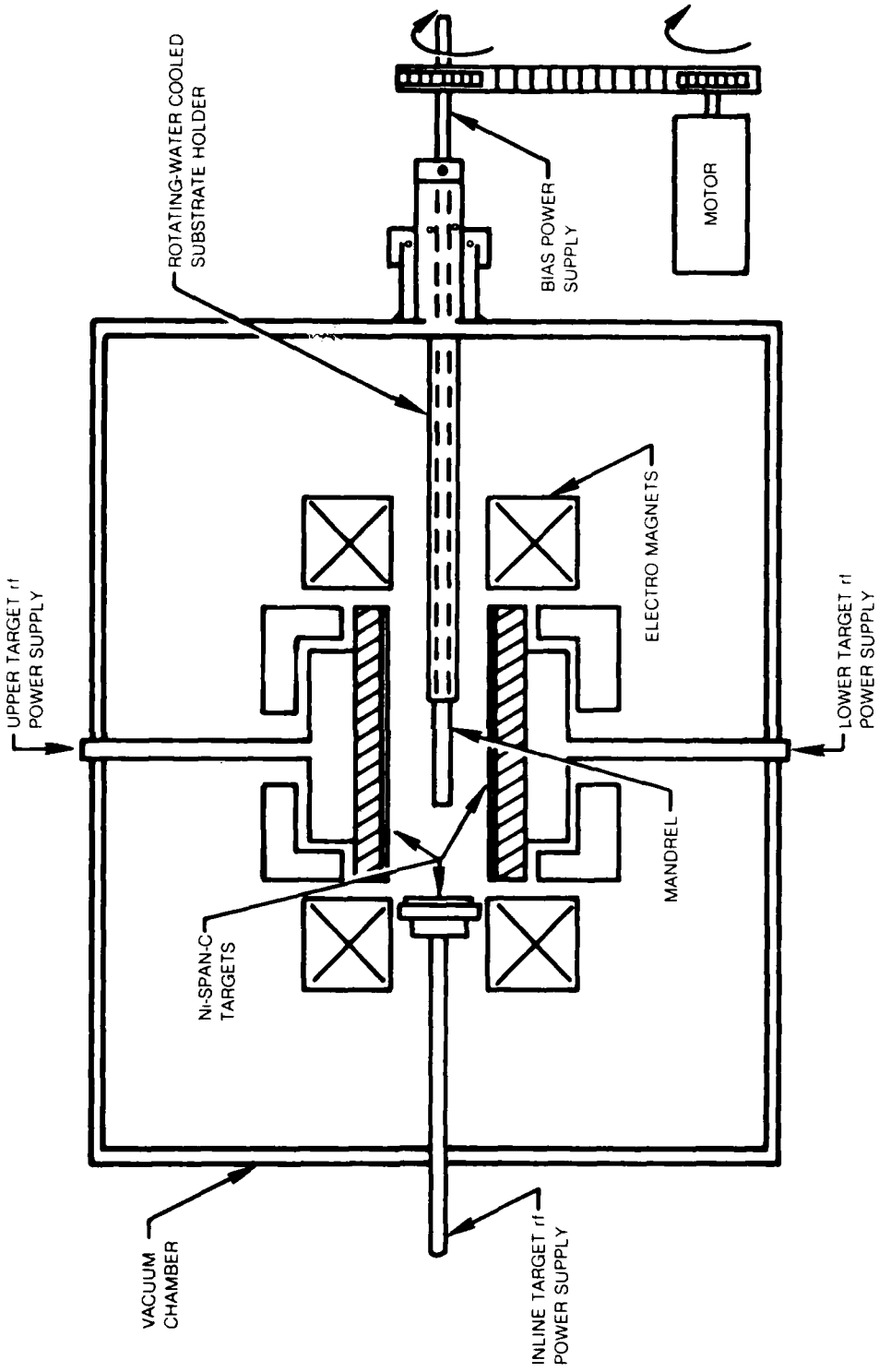

80-8-3-13

FIG. 4

SCHEMATIC OF ALTERNATE SPUTTERING FACILITY

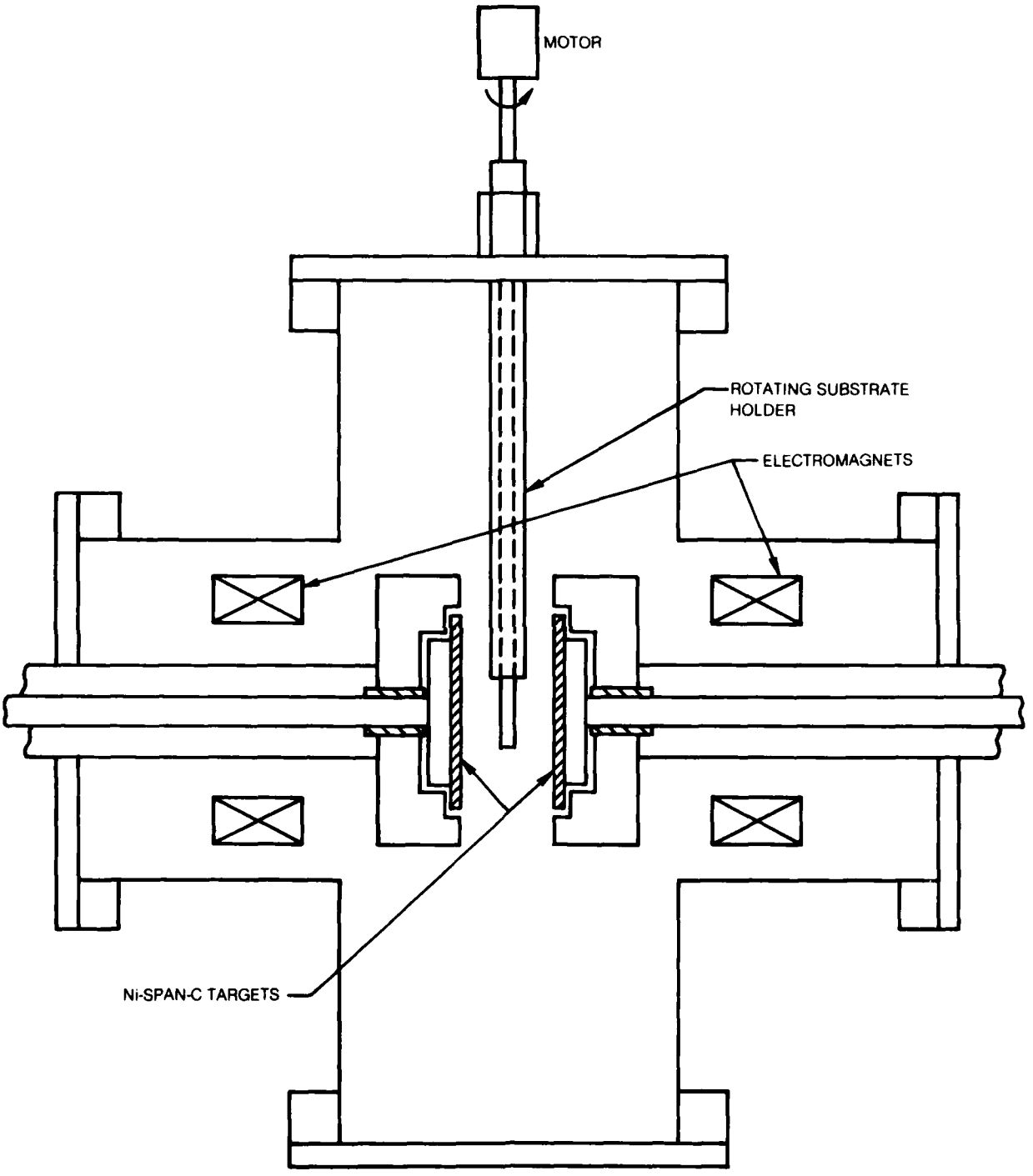

80-8-3-10

2.2 Mandrel Material and Fabrication

Two types of mandrel materials were used in this program. Aluminum was used as a sacrificial mandrel material and stainless steel was used as a reuseable mandrel material. With the aluminum mandrel, the sputtered shell was removed by selectively etching the aluminum away in a sodium hydroxide solution. The shell material, Ni-Span-C, is unaffected by the etch solution. While this approach worked very well for removing the sputtered shell intact from the mandrel, there are disadvantages in using an aluminum sacrifical mandrel. The most obvious disadvantage is that sacrifical mandrels are by definition not reuseable. Therefore, the fabrication cost of the mandrels could become a major consideration in the overall cost of fabricating the part. In our application, the size and surface tolerances of the mandrel required precise machining, resulting in a substantial recurring expense. The use of an aluminum mandrel also imposed a relatively low deposition temperature limit because of its low melting point. Because of these limitations, it was decided early in the program to try to find a reuseable mandrel which was capable of sustaining higher deposition temperatures.

Reuseable mandrels were made of 300 series stainless steel. In order to facilitate removal of the sputtered shell, the stainless steel mandrels were covered with a parting layer before deposition began. Various materials were tried as parting layers. For example, in some cases the stainless steel was simply lightly oxidized in air before deposition. Alternatively, the mandrels were coated with mineral oil and the oil carbonized by heating in air. By far the most reliable method, however, was to overcoat the mandrel with a few tenths of a micron of sputtered SiO_2. This provided a smooth uniform coating on which the Ni-Span-C did not adhere well. Furthermore, it was found early in the program that shells deposited without some electrical biasing to the substrate were structurally very weak. Therefore, in order to further assist in the removal of the shell from the mandrel, the initial deposition on the mandrel was done without bias. After a suitable thickness of coating had been deposited without electrical bias, the remainder of the shell was deposited with the bias applied. Removal of the sputter-formed shell could then generally be easily accomplished after some mechanical working of the coated mandrel. Typically, the mechanical cold working consisted of burnishing the sputtered shell with a steel wire brush as the coated mandrel was rotated, followed by glass bead peening for several minutes. At this point, the shell could generally be easily removed from the mandrel with the mandrel left intact to be used again.

If mechanical cold working of the shell was not desired, the shell could be removed by utilizing the differences in thermal expansion coefficients between the shell and the mandrel. Since the coefficient of thermal expansion of Ni-Span-C is about half that of stainless steel, the mandrel can be shrunk away from the shell by greatly reducing the temperature. A convenient means of doing this consists of plunging the coated mandrel in liquid nitrogen.

All mandrels were fabricated by precision machining to the tolerances specified for the Hamilton Standard Vibrasense^{R} vibrating cylinder pressure transducer. The mandrels were all threaded internally so that they could be screwed onto the half inch diameter shaft which rotated the mandrel in front of the sputtering targets. Figure 5 illustrates a typical stainless steel mandrel used in this program along with the shell which has been sputtered onto it.

2.3 Deposition Process

The deposition process consisted of sputtering Ni-Span-C from rf planar diode cathodes onto the rotating mandrel. The angular velocity of rotation was about 10 revolutions per minute. The sputtering gas was argon, although some 2 percent CO doped argon was also used in an effort to improve the film quality. After pumping the chamber to high vacuum (10^{-6} torr), the sputtering gas was introduced and the plasma ignited. Normally no bias was applied to the substrate during the initial stages of the run since, as was mentioned in Section 2.2, the unbiased layer aided in the releasing of the shell from the mandrel. After the bias was applied, the deposition was allowed to proceed until the required shell thickness was achieved. Proper shell thickness was achieved by using a time-rate method where the rate for a given set of deposition parameters had previously been determined.

The two major process problems associated with the long high power sputtering runs required to form the thin wall cylinders were:

1. Coating of the fixtures in the deposition chamber.

2. High frequency of target replacement due to rapid target erosion.

Both of these phenomena had been anticipated before the program began, however, the amount of time required to cope with these problems had not been fully appreciated. Of the two, the first problem was the most serious. Despite the guard rings and shields that were devised to prevent electrical shorting due to film build up, the film build up was so great during the long high power runs that shorting or flaking did sometimes occur. As a minimum precaution, it was required to strip all of the fixtures in the vicinity of the target or substrate of any deposit from previous runs before attempting another run. This did not guarantee, but did minimize the likelihood of having to abort the run due to an electrical short developing. It did occur on several occasions that a strip of deposited Ni-Span-C would lift from a grounded metal shield and bridge a half inch gap to the target and short it out. This problem would require further attention in building up a production system.

The second problem resulted mostly from target availability. Only thin (.05 in. thick) sheet Ni-Span-C stock was available for this program. As a result,

FIG. 5

SPUTTERED THIN WALL CYLINDRICAL SHELL AND STAINLESS STEEL MANDREL

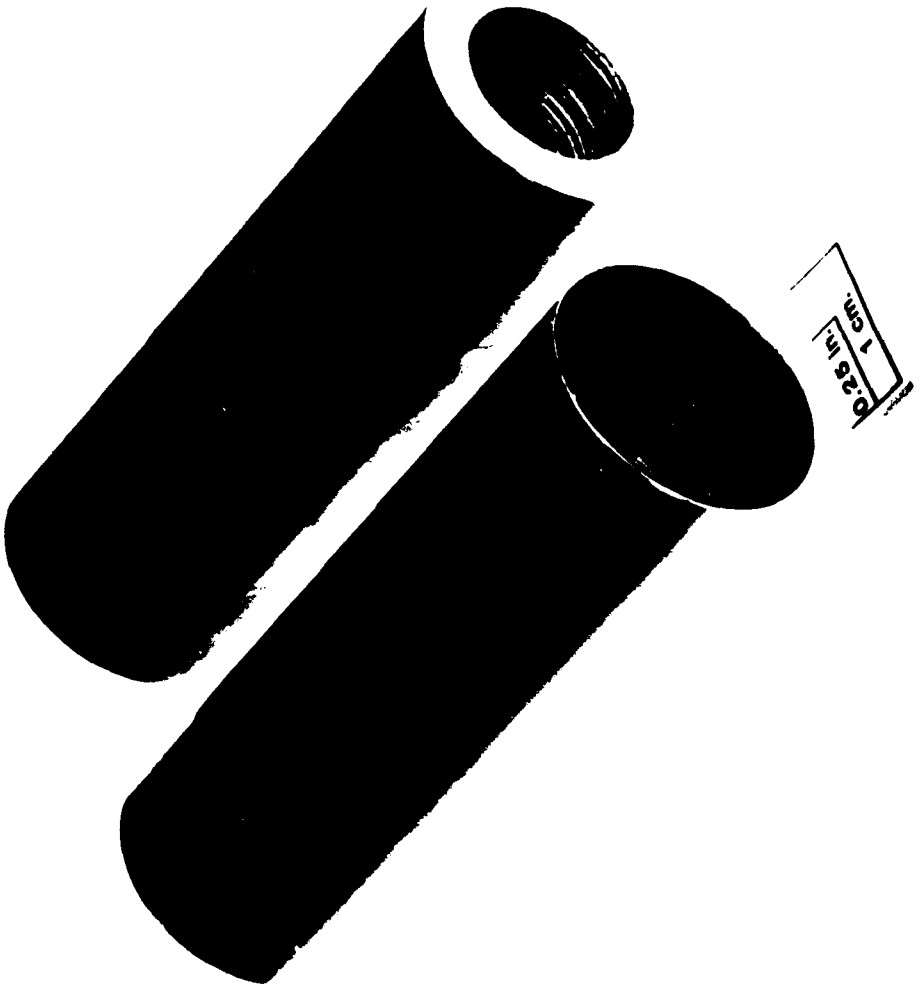

79-125-C

80-8-3-2

these targets eroded through quickly and had to be replaced often. An obvious solution to this problem would be to procure thicker target stock by special order from the producer. A special order for this program would have resulted in an intolerable time delay as well as a huge surplus of material. However, it is felt that the need for continual target replacement was detrimental to achieving consistent shell quality.

The deposition parameters which were available for controlling the process and the resulting metallographic structure of the shells were:

1. Sputtering gas - pressure and type
2. Deposition rate
3. Substrate temperature
4. Substrate bias
5. Magnet field strength.

Sputtering Gas

The sputtering gas used in this program was for the most part 99.999 percent pure argon. A 2 percent doped CO argon gas was used for some runs where it was felt that the CO would combine with any residual oxygen in the sputtering system. This in turn would result in a cleaner deposited film. However, there was no evidence that the doped gas improved the structure of the film.

The gas pressure typically was at 10 m torr. Variations in pressure included the range between 3 m torr and 15 m torr. Film quality was good for the pressure range between 5 and 10 m torr. Gas pressures below 5 m torr resulted in unstable operation. Gas pressure above 10 m torr resulted in a more open structure.

Deposition Rate

Deposition rates ranged from about 1 micron per hour to about 8 microns per hour. Acceptable shells could be made at all of these deposition rates. However, the best thin wall shells were formed at the higher rates; from 5 μm per hour on up. This is fortunate since the higher rates resulted in a shorter deposition time. Even so, at 5 μm per hour, the deposition time to form a .0025 inch thick shell is 12.7 hours. While this may seem to be a long time to fabricate one shell, it must be remembered that an operator is not required to be in continuous attendance at the sputtering machine, but rather he can be occupied doing other tasks once the deposition process has started. Furthermore, for a production application, many shells could be formed at once in one sputtering facility.

Substrate Temperature

Substrate temperature during shell formation varied from 290°C to 650°C. Shells grown at the higher temperatures were considerably improved in mechanical properties compared to those grown at the lower temperatures. However, grain size remained small and the sputtered material was more brittle than the bulk. Figure 6 shows the typical grain formation of one of the best shells grown. No past deposition treatment was performed on this sample. For comparison, a polished and etched sample of bulk Ni-Span-C is also shown in Fig. 6. Note that the grain sizes of the bulk sample are up to about 40 times larger than those of the sputtered material. Note also that a change in grain size and crystallographic morphology occurred when the deposition process was interrupted. However, when the process was restarted, the normal grain growth resumed.

Substrate Bias

By far the most significant deposition parameter affecting crystallographic growth of the sputtered shells was the substrate bias. As might be expected, achieving the proper crystallographic morphology in the sputtered shells was one of the major problems to be addressed in this program, since the performance of the shells depdnds to a large extent upon specific mechanical properties. Figures 7A through 7J are fracture sections and polished microsections of Ni-Span-C. In Figs. 7A and 7B are shown sections taken from a bulk sample of Ni-Span-C. Note that the fractured surface shows no preferred grain shape or size. Note also that the surface is very irregular showing no preferred direction for the fracture to occur. This fracture is characteristic of the type exhibited by a ductile material. In the polished and etched section of the bulk sample, the grain pattern is indicative of equiaxed growth. Figures 7C through 7J are sections of sputtered shells deposited under various conditions, with the exception that the deposition temperature was maintained at 650°C. Figures 7C and 7D are sections of a sputtered Ni-Span-C shell deposited with a negative dc bias of 100 V at a rate of 1.6 μm/hr. The structure of this sample is fairly uniform as seen in the polished section but the fracture section shows a tendency toward columnar growth. The shell was brittle and easily fractured. Figures 7E through 7H are sections of a Ni-Span-C shell deposited with a 150 V negative dc bias at a rate of 1 μm/hr. In these sections, it appears that all traces of preferred orientation have been removed by this bias. However, the nature of the fracture indicates a high degree of brittleness since, as can be seen, the break is smooth and clean as opposed to the more flowed surface of the bulk specimen. Figures 7E and 7F are sections of the as-grown film, while Figs. 7G and 7H are sections of the same film after glass bead peening. There is no evidence in the fracture sections that the glass bead peening has altered the structure; however, in the polished and etched samples, the grains appear to have been compressed due to the peening. Figures 7I and 7J are sections of samples deposited with the same 150 V negative dc bias but at a rate of 3 μm/hr. This growth rate is aprpoximately three times faster than that of Figs. 7G and 7H. This final sample shows a fracture

FIG. 6

GRAIN STRUCTURE OF Ni-SPAN-C

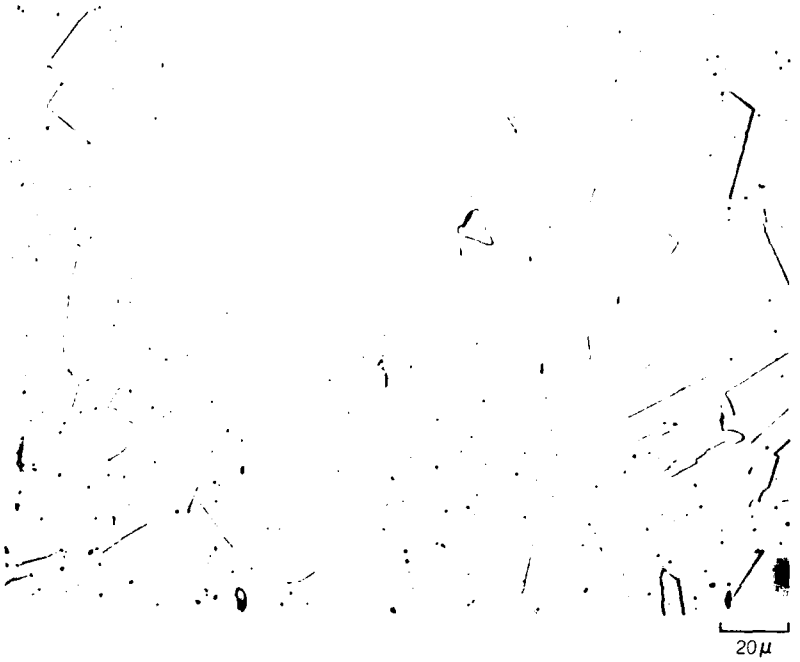

BULK MATERIAL
POLISHED AND
ETCHED

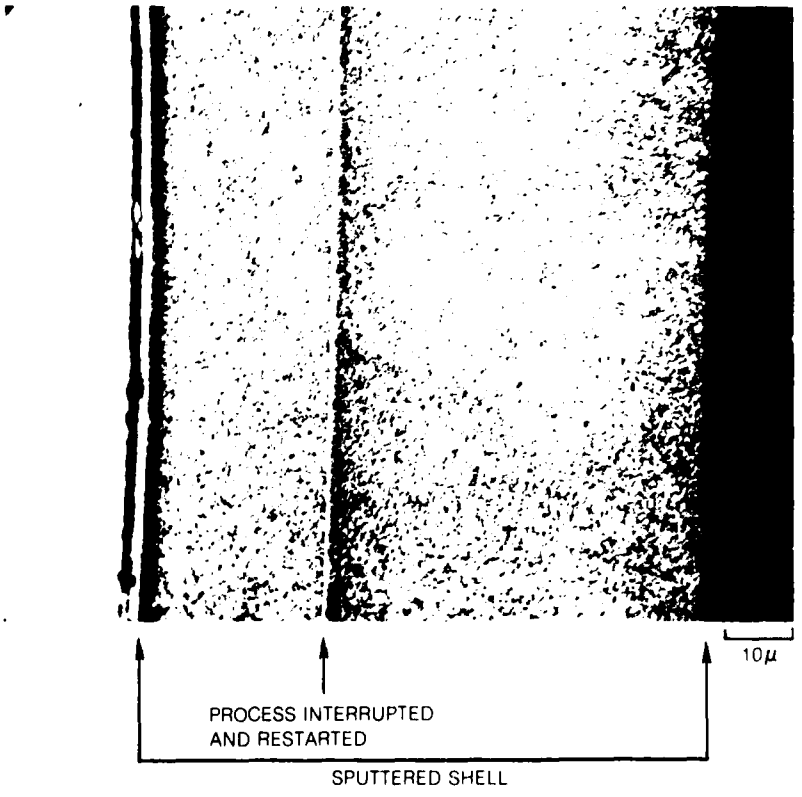

SPUTTERED AT
5.4 μm/hr
650°C
POLISHED AND
ETCHED

80-8-3-6

FIG. 7

FRACTURED AND POLISHED SECTIONS OF Ni-SPAN-C

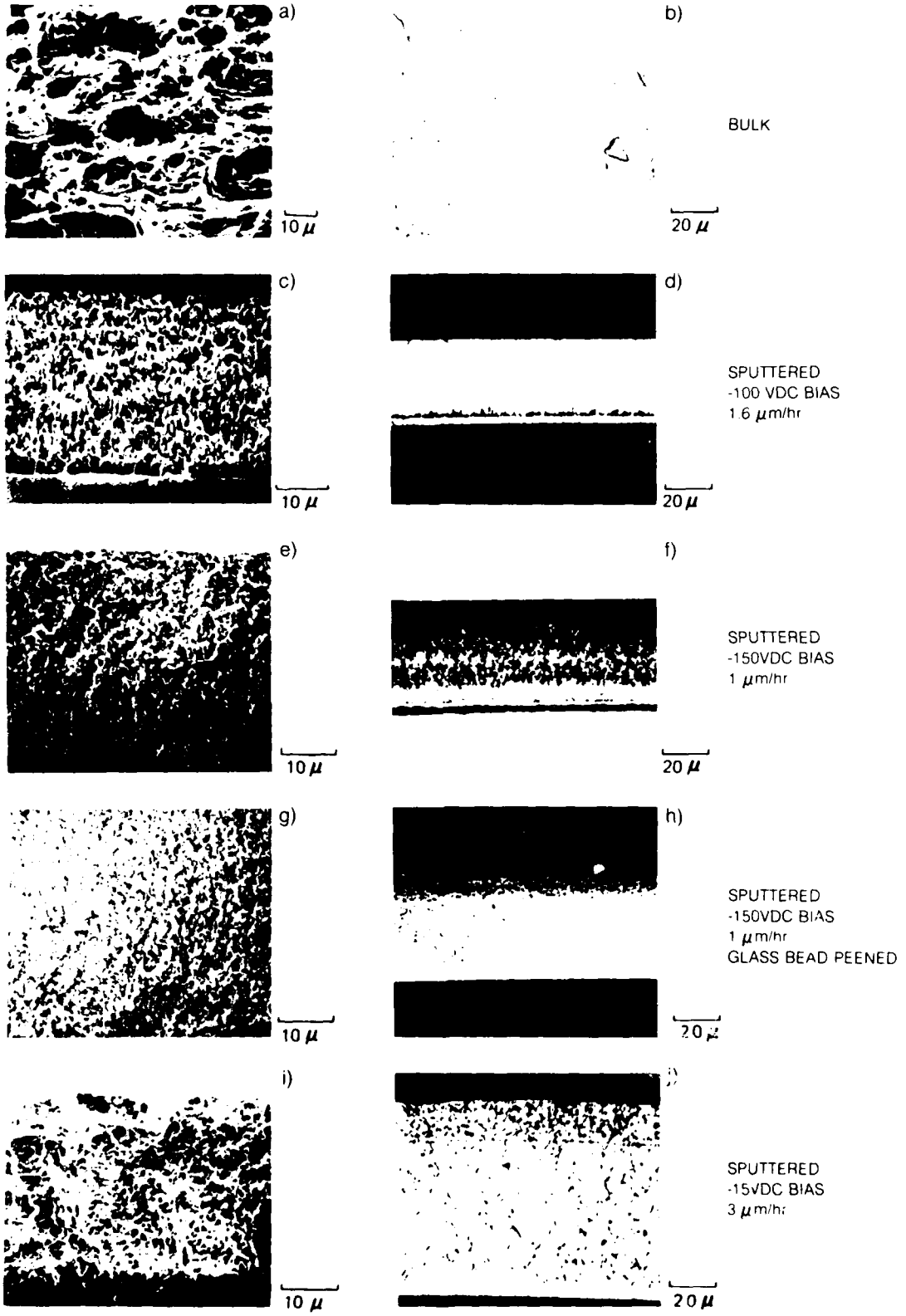

80-8-3-3

pattern much closer in nature to the bulk sample than any of the others. Note that the surface shows that the metal has a tendency to flow before fracturing which is more characteristic of ductile material. In fact, this sample exhibited a greater resistance to fracture than did any of the other sputtered samples.

It is postulated that the higher deposition rate was beneficial to the mechanical properties of the shell because less gas and few impurities could become entrapped during sputtering. Because of the presence of reactive metals such as Ti, Al and Fe in Ni-Span-C, impurity gases such as oxygen and water vapor could be particularly harmful.

With the exception of the bulk sample all of the sputtered samples discussed above were subsequently heat treated at 1050°C in hydrogen for 2 hours. Except for a slightly greater resistance to fracture, no pronounced improvement in ductility of the samples was noted as a result of the heat treatment. Fracture samples examined under the scanning electron microscope also showed no noticeable change in structure from the unheat treated samples. From these observations, it is further postulated that impurity gases in the sputtering system or impurities trapped during the growing of the films could form oxides or other compounds with the reactive metal components of the alloy and act as pinning sites for the fine grains. This would inhibit equiaxed grain growth even under high temperature heat treating.

Magnetic Field Strength

In addition to the deposition parameters discussed above, magnetic field strength in the vicinity of the targets was also investigated. The magnetic field produced by the electromagnets surrounding the targets was varied from zero to 400 Gauss. Shells grown with zero or low magnetic field strength were structurally poorer than those grown with a field strength between 100 and 300 Gauss. The best shells were formed with magnetic field strengths of 300 Gauss.

2.4 Sputtered Ni-Span-C Composition

Ni-Span-C is a complex nickel-iron alloy. In addition to nickel and iron, Ni-Span-C has chromium and titanium in its composition which make it an alloy with a controllable thermoelastic coefficient. This property is used in the design of the Vibrasense^{R} vibrating cylinder pressure transducer to temperature compensate the instrument. Since the coefficient of thermal expansion is positive and since the thermoelastic coefficient can be adjusted to a predetermined negative value, the change in vibrating frequency of the cylinder as a function of temperature can be made vanishingly small. However, the complexity of the alloy adds to the difficulty not only of depositing it in the proper composition but also of achieving the required crystallographic structure.

The limiting chemical composition, the analyzed composition of a target, and the analysis of a deposited shell from the same target are shown in Table 1. Note that while there are some minor variations in the deposited shell composition with respect to the target composition, the composition of the shell is, with the exception of titanium, within the range specified for the limiting compostion. Therefore, from a compositional point of view, the sputtered shell is truly Ni-Span-C.

It should be pointed out that in analyzing the sputtered shell composition, care must be exercised in interpreting the results based on the type of post deposition treatment that the shell has seen. For example, when the shells were formed on sacrificial mandrels, they were removed by etching the aluminum away in a sodium hydroxide solution. Since the method of analysis used to determine composition was the electron microprobe which is very resistive to surface contamination, the results showed a higher aluminum content than was allowed in the limiting composition. Similarly, one method of removing the shells from the stainless steel mandrels was to cold work them slightly by burnishing them with a stainless steel brush. When these shells were analyzed for composition, they showed an abnormally high iron, nickel, and chromium content and a depressed aluminum and titanium content, apparently from a transfer of stainless steel onto the surface of the shell. The analysis in Table 1 is of a sputtered shell that has had no post deposition treatment other than being plunged into liquid nitrogen to remove it from the mandrel.

2.5 Sputtered Shell Thickness Uniformity

Thickness uniformity of the sputtered shell was a mechanical requirement of the Vibrasense^{R} pressure transducer which had to be met. Nonuniformities in either the axial or circumferential direction would result in unstable and unpredictable operation of the vibrating cylinder. In the laboratory shell fabrication system, the targets were 5 inches in diameter. The length of the sputtered shell was approximately 1.87 inches long. The mandrel onto which the shells were formed was also 1.87 inches long and approximately 0.70 inches in diameter. The target to mandrel distance was approximately 2.5 inches. Shell thicknesses were required to be $0.0025 \pm .0001$ inches. Figure 8 is a plot of the thicknesses measured on a typical sputtered shell. These measurements were made from a mounted polished section using a calibrated optical microscope. As can be seen, the sputtered shell thickness uniformity was well within the specified tolerances for the machined shell.

2.6 Thin Wall Cylindrical Shell Pressure Transducer Elements

Having been successful in forming a thin wall shell by sputtering, it became necessary to form a thin wall shell which could be used as a vibrating cylinder pressure transducer element. The final assembly required of a thin wall element for use in the Vibrasense^{R} is shown in Fig. 9. Note that relatively heavy sections

SPUTTERED SHELL THICKNESS

(ALL DIMENSIONS IN INCHES)

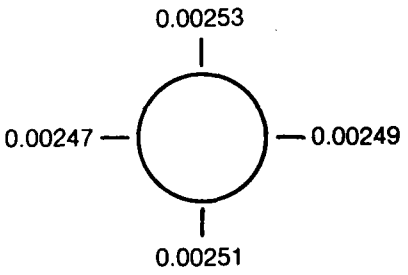

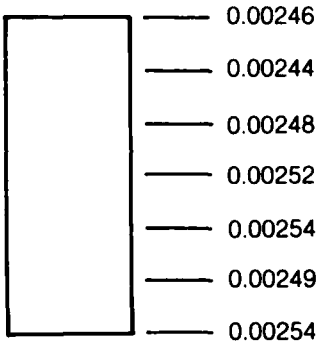

80-8-3-1

HSD VIBRATING CYLINDER

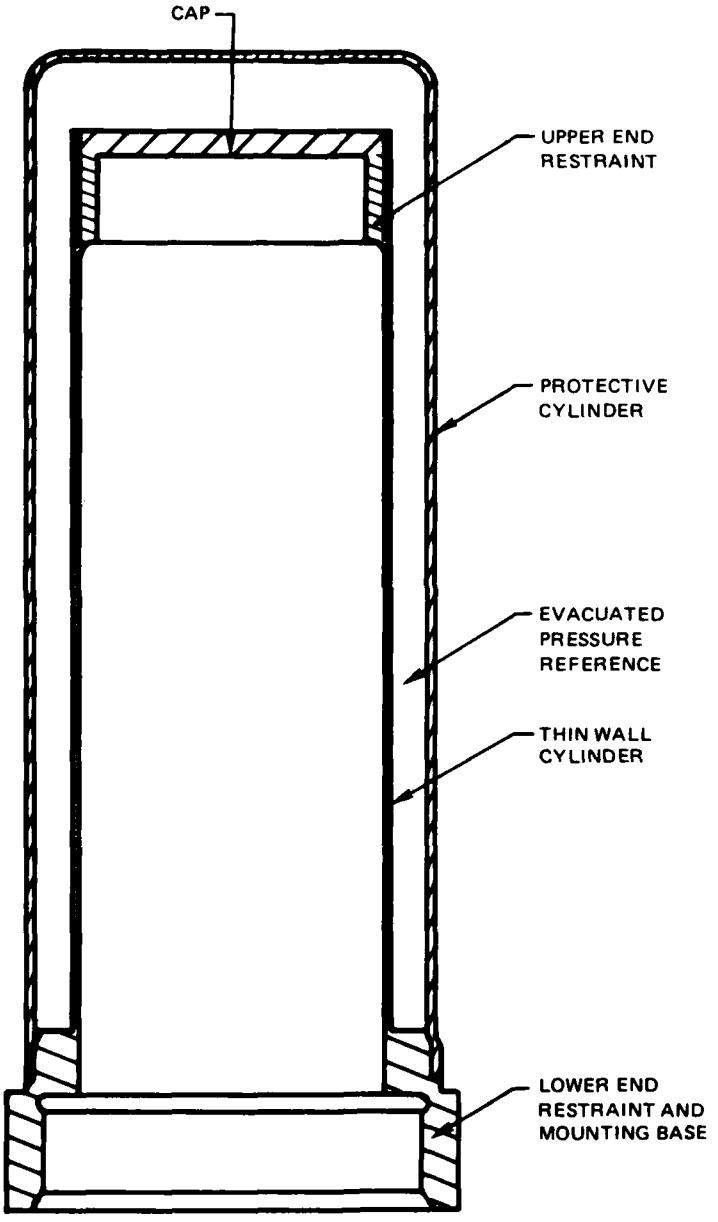

79-05-32-2

TABLE 1

ELEMENTAL COMPOSITION OF NI-SPAN-C

Element	Limiting Composition %	Target Analysis	Shell Analysis
Nickel	41.0 - 43.5	43.9	42.3
Chromium	4.90 - 5.75	5.60	5.22
Titanium	2.20 - 2.75	2.91	3.15
Aluminum	0.30 - 0.80	0.43	0.51
Carbon	0.06 Max	---	---
Manganese	0.80 Max	---	---
Silicon	1.00 Max	---	---
Sulfur	0.04 Max	---	---
Phosphorus	0.04 Max	---	---
Iron	47.3 - 51.6	47.2	48.9

are attached to each end of the thin wall section. The upper-end restraint is used not only to provide a sturdy member to attach the vacuum tight end cap, but also it provides a mechanical ground for the vibrating thin walls. In this way, a nodal point exists at the lower edge of the upper end restraint. In a similar way, the lower end restraint also provides a nodal point at the opposite end of the thin wall section. Furthermore, the lower end restraint must provide a sturdy mechanical base to mount the cylinder to its mechanical package. In this program three different schemes were tried to fabricate a thin wall cylinder for use as a pressure sensing element in the Hamilton Standard Vibrasense^{R} Vibrating Cylinder Pressure Transducer.

The first scheme that was tried and which ultimately was the most successful was to fabricate a simple thin wall open ended cylinder as shown in Fig. 10. Then using a conventionally machined end cap and mounting base, the cap and the base were electron beam welded to the thin wall shell to form a complete unit as shown in Fig. 11. A conventionally machined cylinder is also shown in Fig. 11 for comparison. Details of this assembly are shown in Fig. 12. This construction satisfied all of the mechanical criteria for the pressure element, but because of the necessity of machining the end pieces in addition to the welding, the cost of fabrication was not reduced as much as desired.

In another method of construction, the end restraints were premachined from bulk Ni-Span-C. The mandrels were fabricated with accurately machined recesses at each end such that when the end restraint pieces were slid onto the mandrel into these recesses, the mandrel again appeared to be a solid cylinder. However, in preparing the mandrel for sputtering only the stainless steel portion was coated with the release film. In this way, it was anticipated that the sputtered shell would adhere sufficiently well to the Ni-Span-C end restraint rings to form an essentially continuous construction. This would eliminate the need for welding in the final construction. The problem with this approach turned out to be the difficulty in forming a continuously smooth surface for the shell to grow onto. Precise machining, deformable filler material and mechanical force were all used in an attempt to maitain a continuously smooth mandrel surface. However, in spite of all of these efforts, the shell always remained weak in the region where the stainless mandrel and the end restraint caps were in contact. Figure 13 shows a mandrel configuration with an end restraint cap. An enlarged view at the end cap-mandrel junction shows the type of weakness which was manifested in the sputtered shell as a result of this type of construction.

The third method of construction that was tried consisted of sputtering the complete shape of the vibrating cylinder to include the end cap and base configuration as well as the cylindrical walls. This was done as one complete sputtering operation and removed from the mandrel in one complete unit. Figure 14 shows such a continuous shell together with the mandrel on which it was formed. However, it was still required to have rugged end restraints to perform the function of

FIG. 10

SPUTTERED THIN WALL Ni-SPAN-C CYLINDRICAL SHELL

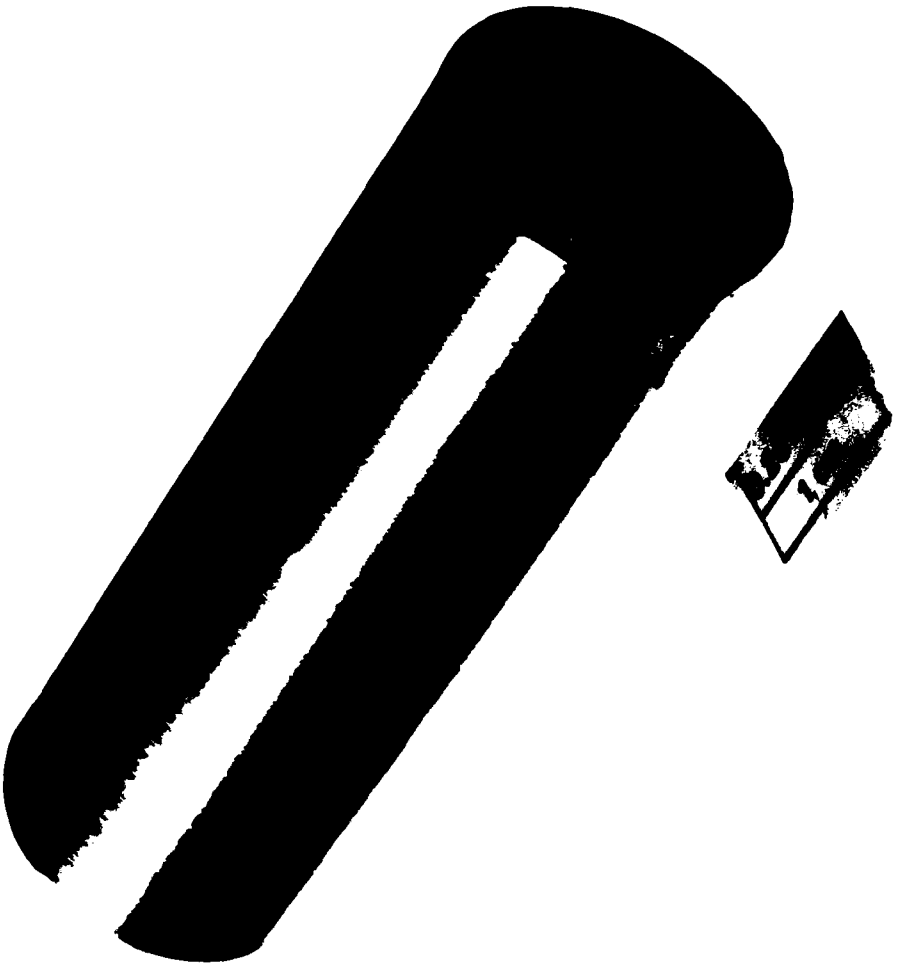

78-349

78-10-320-1

CONVENTIONALLY MACHINED THIN WALL CYLINDER (A), SPUTTERED THIN WALL CYLINDER WITH MACHINED END PIECES (B)

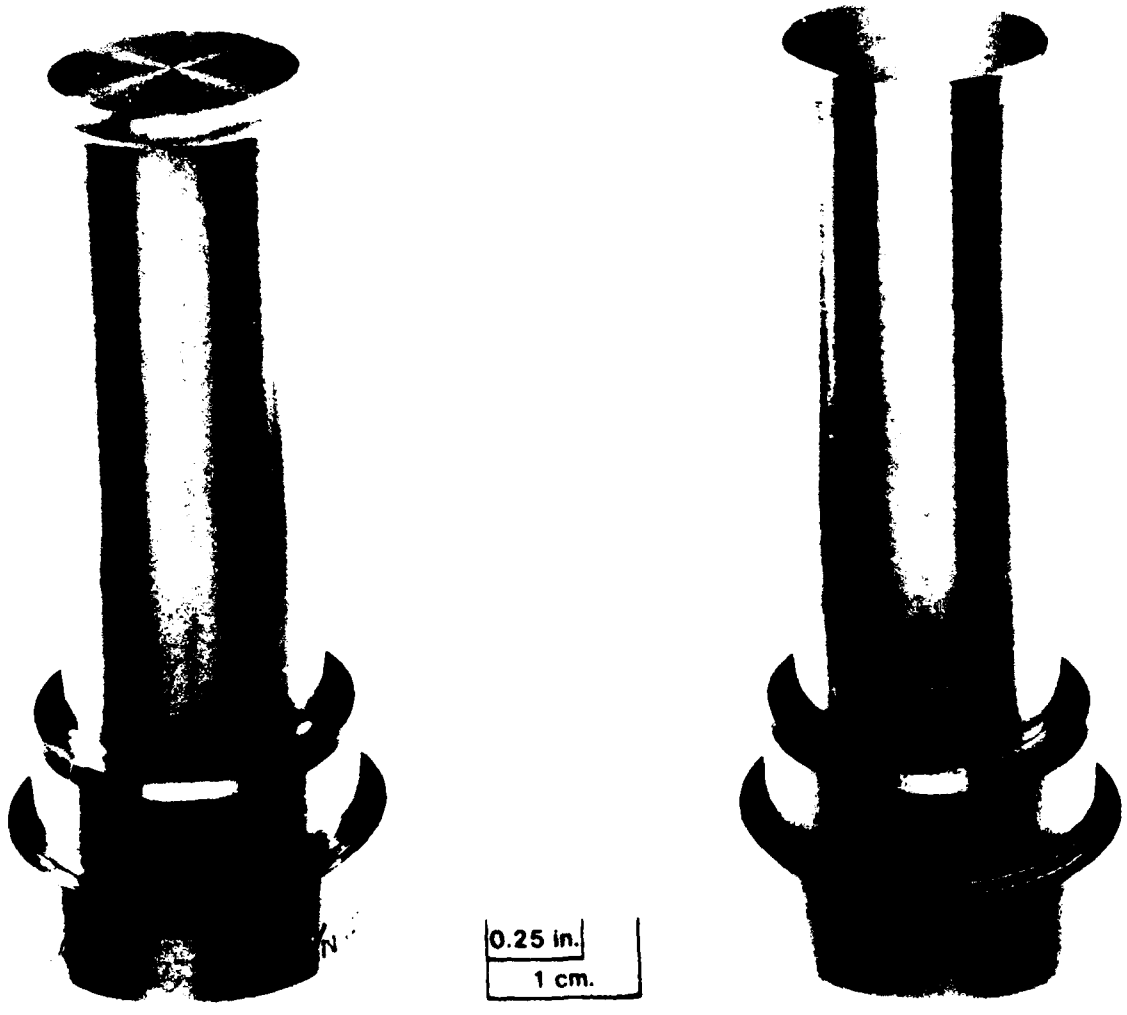

a) b)

FIG. 11

FIG. 12

COMPONENTS USED TO BUILD UP A VIBRATING CYLINDER UNIT FROM A SPUTTERED SIMPLE CYLINDER AND MACHINED END RESTRAINT PIECES

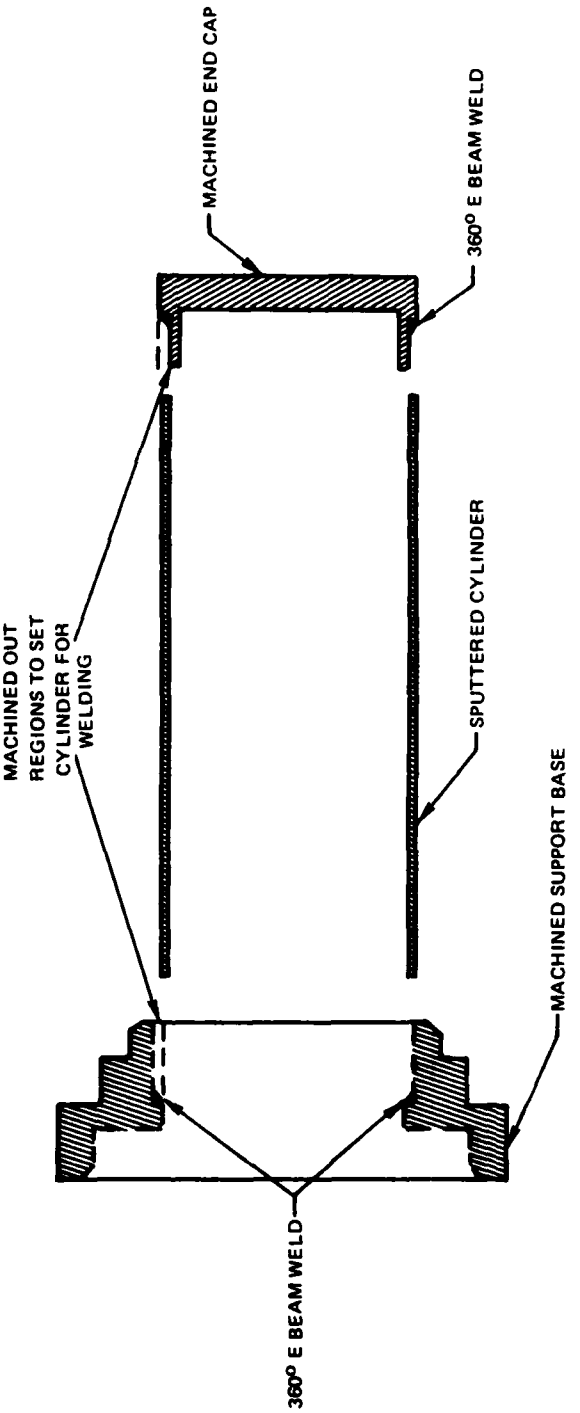

79-08-60-2

FIG. 13

MANDREL ARRANGEMENT FOR SPUTTERING CYLINDERS DIRECTLY ON Ni–Span–C END CAPS

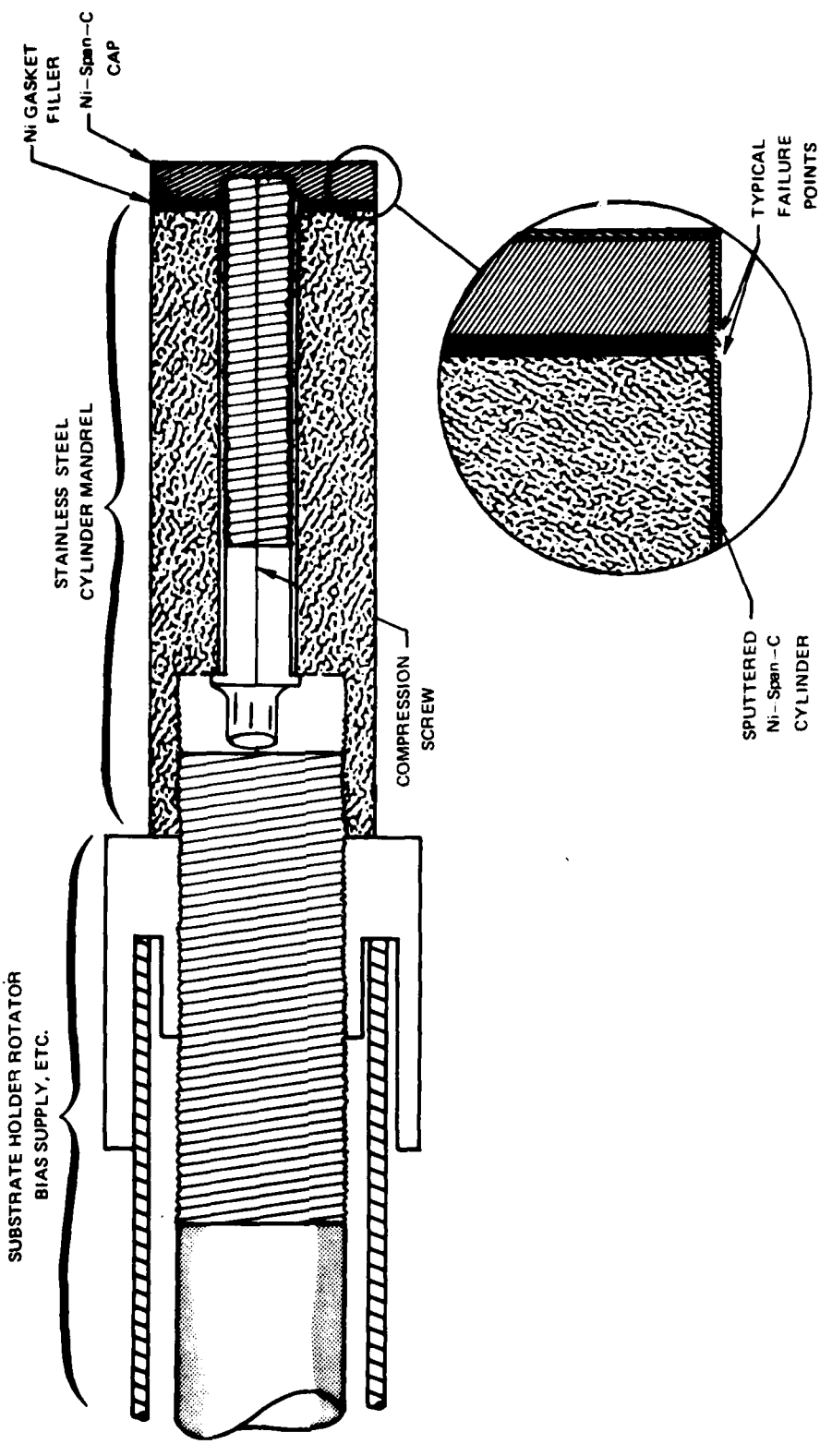

79–08–60–1

FIG. 14

STAINLESS STEEL MANDREL (A), AND COMPLETELY SPUTTERED Ni-SPAN-C SHELL (B)

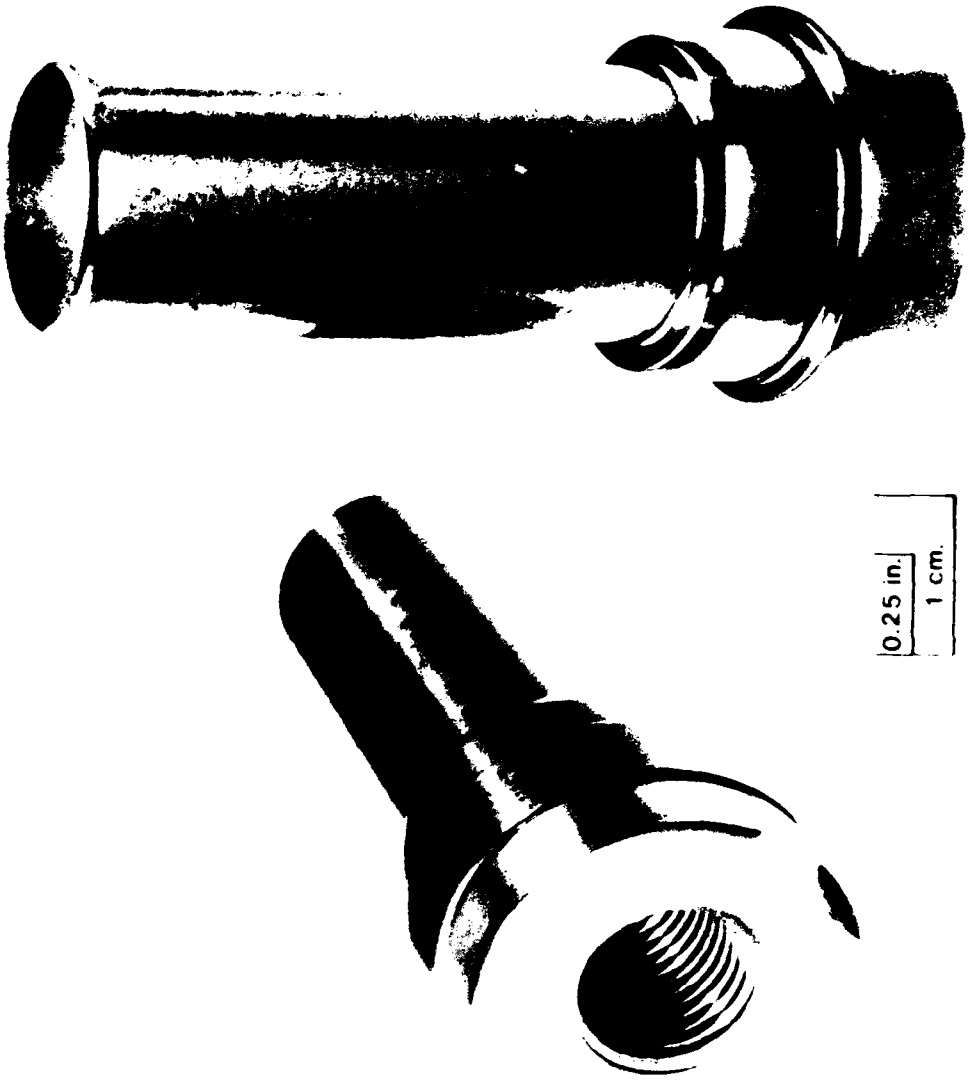

80-95-8

80-8-3-5

mechanically grounding the thin walls and providing a sturdy support base. Figure 15 shows the method planned for attaching the end restraints to this type of sputtered cylinder. However, this construction was never implemented because the sputtered shells proved to be too weak in the region where the sharp internal radii were formed. In forming these shells a sputtering target was added to the system which was in line with the long axis of the mandrel to form the end cap and the stepped portion of the base of the shell. This configuration is shown in Fig. 3.

FIG 15

METHOD USED TO ATTACH END RESTRAINT PIECES TO A SPUTTERED COMPLEX VIBRATING CYLINDER SHELL

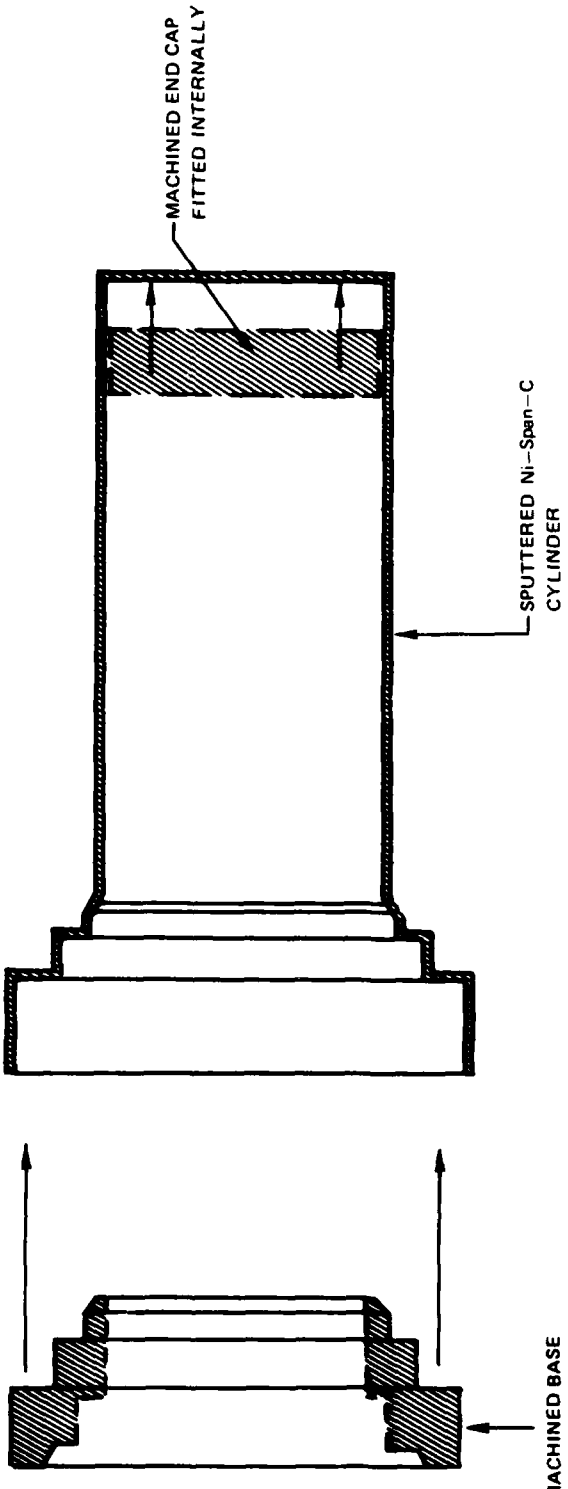

79-08-60-3

3. VIBRATING CYLINDER PRESSURE TRANSDUCER

Thin wall cylindrical shell pressure transducer elements were formed using the first assembly scheme described in the previous section. That is, the thin wall element was assembled by electron beam welding together a sputtered thin wall shell and conventionally machined end cap and mounting base. Several cylinders thus assembled representing the best results of this program were subjected to the Hamilton Standard Vibrasense^{R} tests. All of the cylinders tested vibrated and responded to changes in pressure indicating that they could perform as pressure transducers. However, all cylinders showed a reduced signal output from that seen in the standard machined cylinder. Also, the quality (Q) factor on even the best performing sputtered cylinder was down considerably from that seen on the machined ones. Table 2 below summarizes the results of these tests.

TABLE 2

SPUTTERED CYLINDER PERFORMANCE

	Sputtered Cylinders				Machined Standard
Cylinder No.	1	2	3	4	Cylinder
Frequency of Vibration (Hz)	5338	5338	5691	6009	6400
Output Signal (mv)	17	14	26	20	80
"Q" Factor	--	--	407-1423	1160	9000

Cylinder number 4, which was considered to be the best example of a sputtered vibrating cylinder made in this program, was packaged and delivered to the Naval Air Systems Command as a deliverable item under this contract. This package included the sputtered vibraitng cylinder electron beam welded to the protective outer cylinder as shown in Fig. 9, as well as the associated signal conditions electronics for generating and processing the output signal. A high frequency commercial counter, (Hewlett-Packard Model 5314A Universal Counter) was also provided to detect and display the output signal. A calibration of the pressure input versus the cylinder vibrating frequency output was made for this pressure transducer and the point by point data is shown in Fig. 16. Note that the output frequency is measured to seven significant figures, three decimal places to .001 Hz. It should be noted that the last figure is significant since, with a stable pressure source, the frequency of vibration holds this last place. Figure 17 shows a continuous plot of the frequency versus pressure. The curve is smooth and very nearly linear up to about 49 psia where the cylinder suddenly stops vibrating, restarts again

FIG. 16

CALIBRATION TABLE FOR SPUTTERED Ni-SPAN-C VIBRATING CYLINDER PRESSURE TRANSDUCER

PRESSURE PSIA	FREQUENCY Hz
1	5685.888
2	5710.663
3	5735.194
4	5759.572
5	5783.756
6	5807.673
7	5831.481
8	5855.040
9	5878.376
10	5901.515
15	6014.314
17.5	6068.292
20	6120.775
25	6221.110
30	6321.112
35	6404.262
40	6483.024
45	6858.898
49	6922.475

80-8-3-11

FIG. 17

FREQUENCY OUTPUT VS. ABSOLUTE PRESSURE FOR SPUTTERED Ni-SPAN-C VIBRATING CYLINDER PRESSER TRANSDUCER

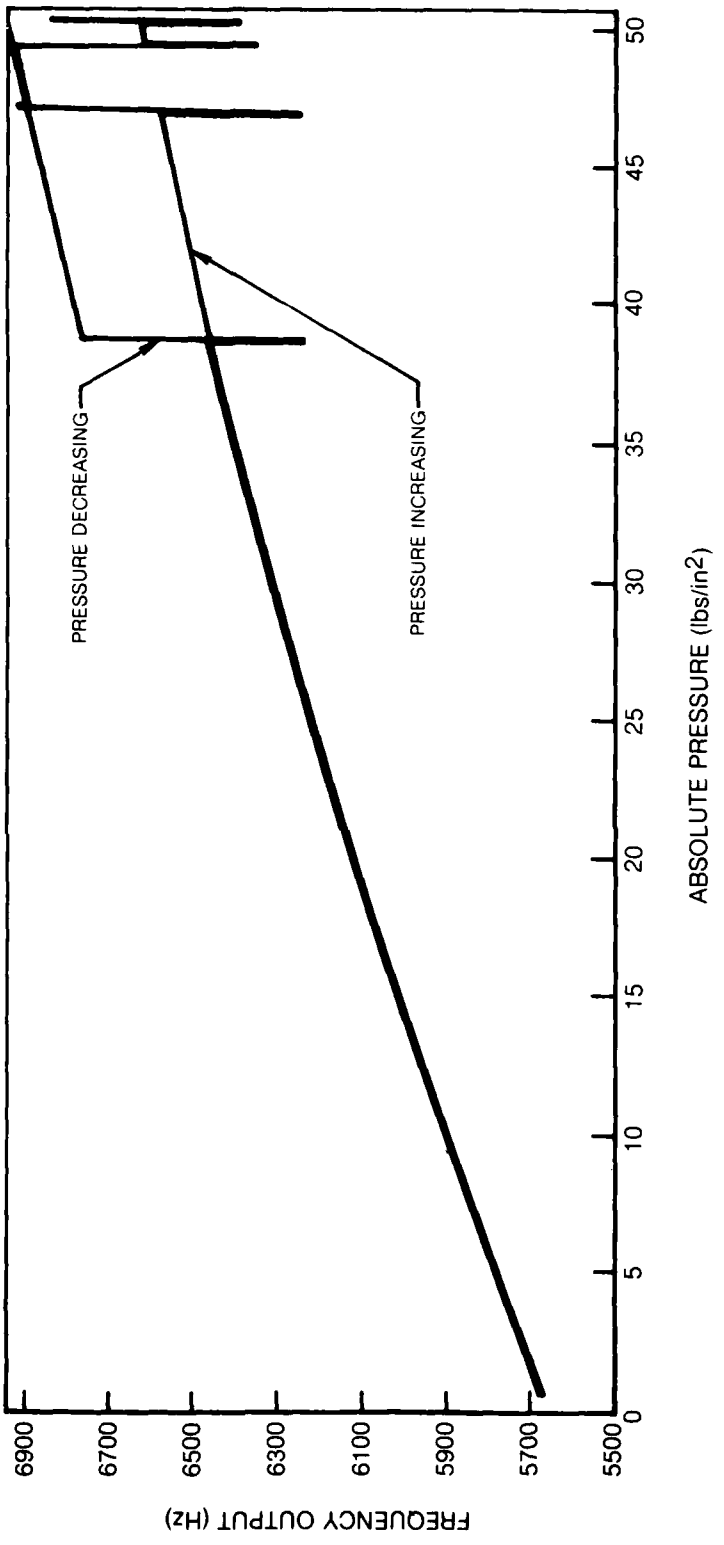

80-8-3-12

just under 50 psia, then stops just over 50 psia. When the pressure is lowered, the cylinder only starts to vibrate again when the pressure has been reduced to about 39 psia after which time it retraces the curve generated with increasing pressure.

The packaged vibrating cylinder and its associated electronics is shown in Figs. 18 and 19. The vibrating cylinder and its electronic package as shown in Fig. 18, was placed in a constant temperature oven at 60°C. The pressure input to the sputtered cylinder was the ambient atmospheric pressure in the laboratory. The same input pressure was fed simultaneously to a temperature regulated vibrating cylinder pressure transducer fabricated by the conventional method by Hamilton Standard. The barometric pressure of the laboratory was thus monitored for 40 hours. The data showed a small but persistent drift of 0.0019 psi/hr for the sputtered cylinder away from the Hamilton Standard Vibrasense^{R} unit. However, the sputtered cylinder did detect the correct variations in the room atmospheric pressure.

It is not known at this time if this drift is due to electronic aging or mechanical aging of the cylinder. Clearly, more work will be necessary to determine the proper aging or heat treating cycle required to stabilize the sputtered shells. The schedule used for the machined cylinders cannot be applied directly.

FIG. 18

VIBRATING CYLINDER PRESSURE TRANSDUCER AND SIGNAL CONDITIONING ELECTRONICS

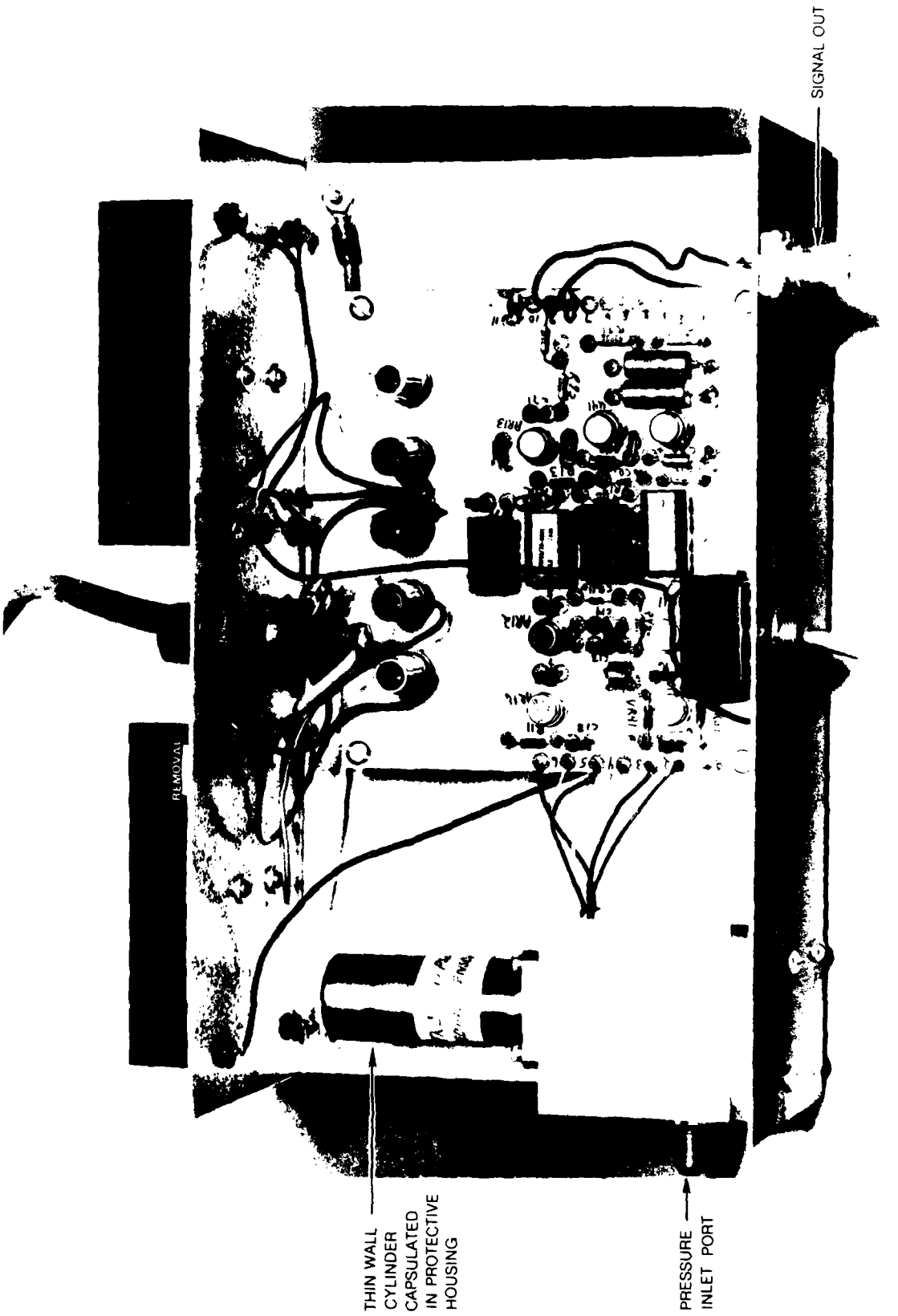

80-266-A

80-8-3-15

FIG. 19

VIBRATING CYLINDER PRESSURE TRANSDUCER, SIGNAL CONDITIONING ELECTRONICS AND FREQUENCY COUNTER

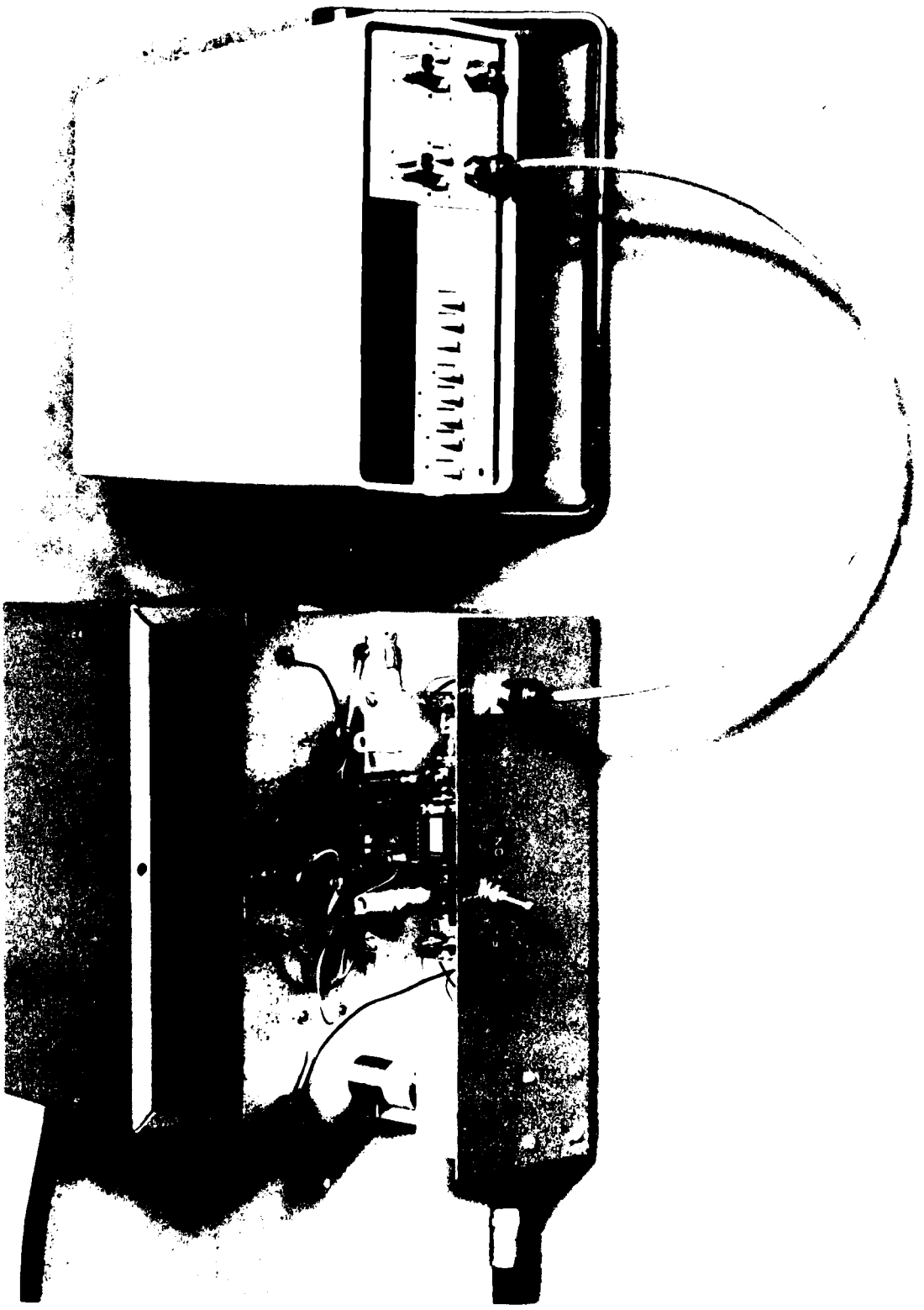

80-266-8

80-8-3-14

4. CONCLUSIONS AND RECOMMENDATIONS FOR FUTURE WORK

In this program it has been shown that thin wall cylindrical shells can be fabricated by sputtering as an alternative to machining. Furthermore, we have demonstrated that sputtered thin wall cylinders can be used as elements in thin wall vibrating cylinder pressure transducers. The best example of sputtered thin wall cylinders produced in this program have not performed quite as well mechanically as have the conventionally machined elements, however. Therefore, more work must be done to further improve the mechanical properties of the sputtered shells.

From the experience gained in this program and from the encouraging results of the assembled vibrating cylinder, it is felt that further work would be justified to refine this technology for manufacturing applications. Though it has not been shown directly in this program, the potential for cost savings in sputtering the cylinders in batch lots as opposed to machining them one at a time is considerable. For example, using a 12 inch diameter planar target system, it is estimated that as many as 30 cylindrical shells could be formed at one time. Assuming a total manpower expenditure of 30 hours per batch for preparation, deposition, post deposition treatment and end restraint assembly, this brings the manpower cost to one man hour per cylinder. Under current production methods, approximately four man hours are needed to fabricate a cylinder.

In a continuing program, the areas which would be investigated would include those which we now feel would have a direct bearing on improving the crystallographic structure of the shells as well as their mechanical properties. As mentioned previously, Ni-Span-C is a very complex alloy with several very active elements, i.e., titanium, aluminum, iron. This could contribute to the difficulty in achieving consistently equiaxed grain growth in the sputtered films because of the high affinity of these elements to form compounds. This hypothesis could be investigated by sputtering shells of successively more complex alloys, starting with a stable single element such as nickel. Subsequent shells would be sputtered of Nichrome, for example, followed by Invar, then Kovar. This type of study would allow us to isolate the process parameters which affect equiaxed growth as more complex alloys with more reactive elements are sputtered. In this way, we would eventually learn to sputter repeatedly good quality Ni-Span-C for shell formation.

Another area which should be investigated is the consistent quality of the bulk target material. As pointed out earlier, one of the problems with conducting sputtering runs of long duration at high power was the rapid erosion of the targets. Since the only Ni-Span-C target material available for this program was .05 inches thick sheet stock, targets had to be replaced after every run. The result of this was that new targets were always being conditioned and the film composition was probably not consistent. In a future program, the target material must be procured in a form large enough to fabricate long lasting targets.

The primary reason for using Ni-Span-C as the vibrating thin wall cylinder material is the fact that its thermoelastic coefficient can be adjusted to a specific value. Since the frequency of vibration is a function of the thermoelastic coefficient and the thermal expansion coefficient, temperature compensation can be achieved by proper choice of the thermoelastic coefficient. In this way, the vibrating frequency can be made independent of temperature changes. The thermoelastic coefficient is adjusted by heat treating the finished machined cylinder according to a schedule based on a specific melt of the bulk Ni-Span-C. However, after the Ni-Span-C has been sputtered, the effect of any previous cold working or heat treatment has been lost. Furthermore, as seen in the table of sputtered Ni-Span-C composition, the results of the analysis of the sputtered material is slightly different than that of the target material. As a result, in order to adjust the thermoelastic coefficient to a specific value, an investigation would have to be conducted with the sputtered material in order to establish the proper heat treating procedure. This type of information should also be sought in any future work in the continuation of this program.

APPENDIX I

A NEW DIGITAL PRESSURE TRANSDUCER

RICHARD C. MEYER
HAMILTON STANDARD
DIVISION OF UNITED AIRCRAFT CORPORATION
WINDSOR LOCKS, CONNECTICUT

Reprinted from the
Proceedings of the
27th Annual Conference and Exhibit
of
The Instrument Society of America

New York, N.Y. October 9-12, 1972

72-601

A NEW DIGITAL PRESSURE TRANSDUCER

Richard C. Meyer

Hamilton Standard
Division of United Aircraft Corporation
Windsor Locks, Connecticut

ABSTRACT

Hamilton Standard is using a new digital pressure measuring concept in their aircraft and industrial systems business. Jet engine fuel controls, air inlet controls, and air data monitoring systems for aircraft will benefit from the use of this stable and accurate device. Industrial users in process control, nuclear plant, and automatic test equipment are also finding that portability, accuracy, and stability now can be obtained in one instrument at a reasonable cost.

This paper discusses the design features of the Hamilton Standard digital pressure transducer. The vibrating cylinder pressure sensing element and its theory of operation are explored—how pressure changes the natural vibratory frequency of the sensing element and how this is converted into an electrical response signal. The many variations of signal output available from the digital transducer are discussed.

A development of the term "accuracy" is presented, followed by an exploration of the detailed accuracy characteristics of the transducer. Approximately 10 different error sources are considered and discussed. These errors are statistically combined to yield an overall accuracy for the transducer.

The packaging philosophy of the transducer and its associated electronics is explained, and a composite photograph of the various models is shown.

Two interesting applications are discussed wherein the transducer was used to make a difficult measurement. One is that of nuclear reactor containment leakage testing, and the other is the use of the transducer in air inlet controls for high performance aircraft.

INTRODUCTION

A demand has been created in the systems business for better transducers. The need comes as a result of ultra-sophistication in the very complex control systems required by modern machines. Much of this complication is the result of having to do the old control job an order of magnitude better because the end item machine either is called upon to be more accurate, more stable, or more responsive. Coupled with this need is the ever present requirement to maintain costs as low as possible.

The trend is quite evident that these exotic systems must be controlled by digital computers. The word "digital" is the key to maintaining the required high accuracy and stability. This cannot be done adequately with analog systems - nor does it have to be.

Years ago, the thought of using digital computers in control systems, especially in hostile environments, was abandoned because of their large physical size, high cost, low reliability, and general delicacy. Now, the situation is different. One can obtain extremely rugged and reliable digital computer hardware at a fraction of its old cost and size. The digital controlled system is now a practical reality. Its increasing popularity has created a demand for complementary digital interface equipment in the form of transducers, analog-to-digital converters, and actuators.

So it was that Hamilton Standard found itself in a major control system competition with an analog pressure transducer that was marginal in doing the job at hand. Thus, the vibrating cylinder digital pressure transducer was elevated from a low level laboratory development study to a high production instrument with a capability to out-perform all other candidates. Tests of the subsequent control system built around this new transducer fully confirm the correctness of adopting this device as the solution to a very difficult systems problem.

The purpose of this paper is to discuss this new concept of measuring pressure, to show how it works, and to explore why it is so unusually stable and accurate. The transducer has many ramifications in terms of output format which lead to a large number of possible applications. We shall look at the physical qualities of the transducer, and then explore the various interesting uses to which it has been put.

THE BASIC TRANSDUCER

Today's digital transducers are available as one of two types:

1) The digital device which generates a time dependent signal such as frequency, events-per-unit-time, pulse width, etc., or

2) the indirect digital transducer which works in an analog format up to the very last stage where the output signal is converted from analog to digital (unusually binary).

The latter indirect transducer is basically analog and shares the problems peculiar to all analog devices such as hysteresis, drift, component tolerance variations, comparator inaccuracies, etc. The better transducers, from an accuracy and stability point-of-view, are the digital devices mentioned in (1) above.

The subject of this paper is a digital pressure transducer of unique design. Its output is a frequency, which can be converted to a binary digital format.

HOW IT WORKS

The vibrating cylinder pressure transducer uses both mechanical and electrical concepts in a closely coupled relationship. However, it is best to separate these two disciplines long enough to discuss their interesting individual characteristics before trying to combine them in a system. So as to make an orderly transition through the transducer system from its pressure input to the output in digital form, let us start with a discussion of the mechanical input stage.

The sensing element consists of an assembly of two concentric closed-end cylinders — a vibrating inner one and a protective outer one. These cylinders are fastened to a common base at one end and are free at the other. A schematic representation of this configuration is shown in Figure 1. An additional central structure is built from the base, and this is called the spool body. The spool body serves as a support for electro-magnets used in (1) exciting or driving the vibrating inner cylinder and (2) detecting its motion and frequency. The space between the vibrating inner cylinder and the protective outer cylinder is evacuated to serve as the absolute pressure reference. The cavity volume between the vibrating inner cylinder and the spool body receives the input pressure, generally through porting passages in the transducer base. A photograph of this assembly is shown in Figure 2.

The side wall of the inner cylinder is excited by magnetic field forces generated with the electromagnetic driver coil located on the spool body. The inner cylinder vibrates at its lowest natural frequency relative to its physical dimensions. This is also its lowest energy level. If we had a very long or open-end, thin-wall cylinder, the lowest hoop mode of vibration that can be excited by the driver coil would have an oval shape. For a relatively short, close-end, thin-wall cylinder, the closed end (boundary) condition causes a different mode shape to form. As the closed-end cylinder is made shorter, the lowest natural frequency becomes higher, as might be expected, but the order of the lowest natural frequency is also higher. This is shown graphically by the curve in Figure 3.

The cylinder configuration used in the pressure transducer is chosen to operate in the four lobed, symmetrical hoop mode shown in Figure 4. This mode shape was chosen because it is easily excited with a bi-polar magnetic drive coil positioned diametrically within the vibrating cylinder. Also, there is greater tolerance to cylinder length variations in the lower numbered orders. The mode shape symmetry also permits the transducer to withstand large acceleration displacements without any loss of magnetic capabilities. This is roughly analogous to changing the resistance in opposite arms of an electrical Wheatstone Bridge circuit in opposite directions and having no net effect.

The magnetic pickup coil is positioned orthogonal to the drive coil in the spool body. The spatial phase relationship helps to start the vibrating cylinder in its four lobed symmetrical mode. It also tends to filter out extraneous pickup because of the nodal symmetry.

The driver coil, the pickup coil, and the mechanically resonant vibrating inner cylinder are interconnected by the flow of electrons through wires and forces created by lines of magnetic flux. A closed loop control circuit is formed by these components, as shown schematically in Figure 5.

With the above as background, a pneumatic pressure can be introduced into the cavity between the spool body and the vibrating cylinder. The wall elements of the cylinder are tensioned by the pressure acting over the cylinder internal area, and this tension causes the cylinder natural frequency to increase as a function of the increased pressure. When the mechanical frequency increases, the magnetic pickup coil immediately detects this and instantaneously relays this information to the amplifier-limiter combination. This new frequency and a new limiting voltage are fed back to the driver coil to produce a reinforcing force pulse at the proper frequency.

The transducer has a natural frequency at its zero pressure point. This is called the transducer offset frequency, or f_o. The change in frequency due to the application of "full scale" pressure, where "full scale" pressure is chosen low enough to avoid stress-creep, results in a frequency change of about 20%.

The expression for pressure as a function of vibratory cylinder frequency is somewhat non-linear, as are most vibratory phenomena. The output equation can be expressed as

$$P = A(f_p-f_o)+B(f_p-f_o)^2+C(f_p-f_o)^3$$

where constants A, B, and C are derived from the calibration of the instrument and f_p and f_o are the transducer frequencies at pressure P and at zero pressure, respectively.

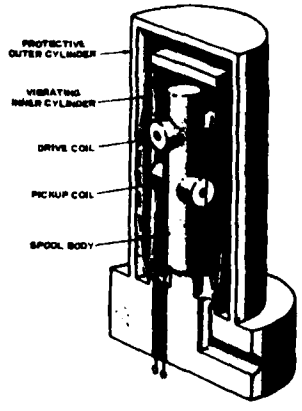

FIGURE 1. SECTIONAL VIEW

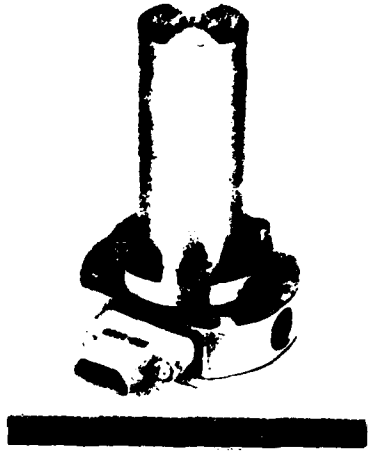

FIGURE 2. VIBRATING CYLINDER PRESSURE TRANSDUCER

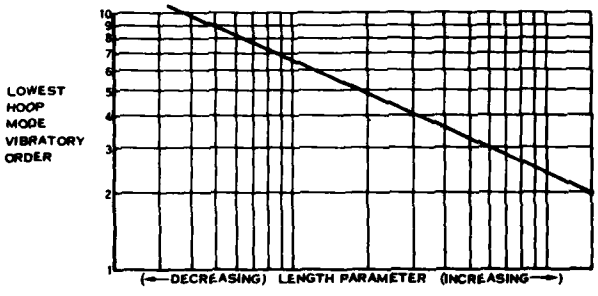

FIGURE 3. LOWEST HOOP MODE VIBRATORY AS A FUNCTION OF CYLINDER LENGTH PARAMETER

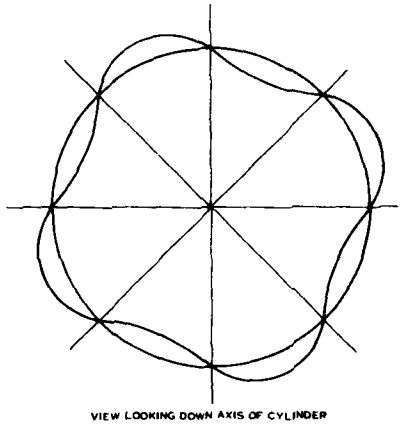

VIEW LOOKING DOWN AXIS OF CYLINDER

FIGURE 4. FOUR LOBED HOOP MODE SHAPE OF VIBRATING CYLINDER

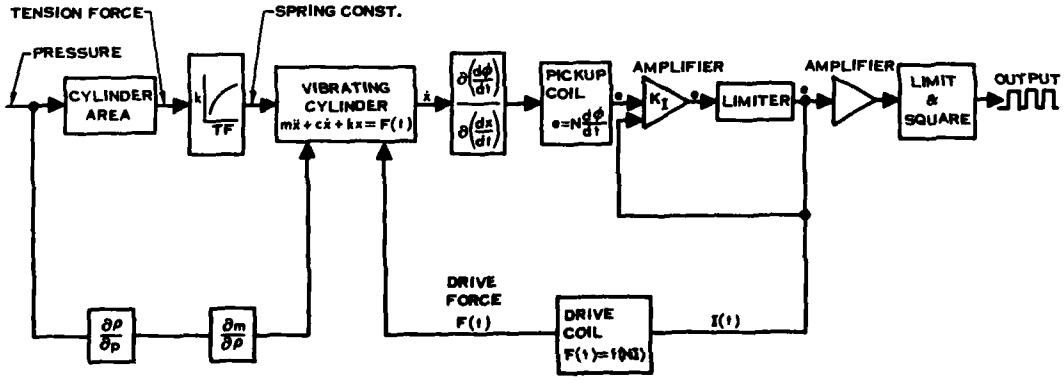

FIGURE 5. VIBRATING CYLINDER PRESSURE TRANSDUCER FUNCTIONAL BLOCK DIAGRAM

TRANSDUCER OUTPUT CONSIDERATIONS

The basic transducer has a 50% duty cycle square wave output signal with a 5 volt amplitude. This signal format is completely compatible with the input/output specifications for digital logic circuitry. The basic frequency signal has infinite resolution.

Although the frequency format has a digital connotation and exhibits the stability implied by this type of device, it is not one normally handled directly by most digital computer or data reduction systems. These systems require a number representing pressure in the binary or binary-coded-decimal (BCD) format. The conversion of frequency into a numerical value with high resolution is usually done by measuring the time or period of a transducer output cycle. A common conversion method is to open a logic gate to a precision, high frequency clock and accumulate the binary count of clock pulses, as they pass through the gate, using a counter. The clock gate is initially opened at the beginning of one transducer output square wave cycle and closed at the beginning of the subsequent transducer output cycle. A number of fixed frequency clock pulses then will have been accumulated in the counter during the time of one transducer output cycle. As an example, suppose the clock frequency is 15 MHz, and the counter accumulation is 3333 cycles for the time elapsed during one transducer cycle. If the accumulated count is divided by the clock frequency, the time lapse is determined. This, of course, is the period of the transducer signal, and for this example,

$$\tau_t = \frac{N_{\mathfrak{C}}}{f_{\mathfrak{C}}} = \frac{3333 \text{ cycles}}{15 \times 10^6 \text{ cycles/sec.}} = 222.2 \times 10^{-6} \text{ sec.}$$

The transducer frequency is the reciprocal of the period, so that

$$f_t = \frac{1}{\tau_t} = \frac{1}{222.2 \times 10^{-6}} = 4500 \text{ Hz}.$$

However, the value of transducer period is the quantity stored in binary form and used later for further computation.

Notice that during that one transducer cycle, a count of 3333 was accumulated. The resolution is 1 part in 3333 or $\pm 0.03\%$. If more transducer cycles are counted, a larger accumulation of 15 MHz pulses would accrue and the resolution would be enhanced. Counting transducer cycles is done with binary logic elements, and it is interesting to see what happens if the clock gate were controlled by, say, $2^6 = 64$ transducer counts. Now, the accumulated count would be $64 \times 3333 = 213312$. A resolution of 1 part in 213312 is obtained or $\pm 0.0005\%$. Recognize, however, that during the longer time required to count 64 transducer cycles to improve resolution, the pressure transducer output is being averaged over a longer time. This reduces the response time of the pressure measurement. As usual, if response of the instrument is increased, accuracy (in the form of resolution) decreases.

The above discussion centers on the determination of transducer frequency or period in a precise manner. But, the determination of pressure is what is really required, and the resolution of measuring pressure must be calculated by considering the difference between the transducer period at the measured pressure and the transducer period at zero pressure. The resolution of pressure is expressed by

$$\frac{1}{N_{\mathfrak{C}}} = \frac{1}{(\tau_o - \tau_p)(f_{\mathfrak{C}})(N_t)}.$$

If values are given to these parameters the resolution of the pressure measurement can be calculated, viz:

$f_o = 4500$ Hz; $\tau_o = 222.2 \times 10^{-6}$ sec.

$f_{20} = 5500$ Hz; $\tau_{20} = 181.8 \times 10^{-6}$ sec.

$f_{\mathfrak{C}} = 15 \times 10^6$ Hz

$N_t = 2^6 = 64$

$$\frac{1}{N_{\mathfrak{C}}} = \frac{1}{(222.2-181.8)\ 10^{-6}\ (15)10^6\ (64)}$$

Resolution is 1 part in 38784 or 0.0026% of 20 psia.

Another possible treatment of the transducer output signal is to use the binary representation of period in a digital computer for the solution of the third order pressure/frequency polynominal equation. In terms of transducer period, the equation is

$$P = A\left(\frac{1}{\tau_o} - \frac{1}{\tau_p}\right) + B\left(\frac{1}{\tau_o} - \frac{1}{\tau_p}\right)^2 + C\left(\frac{1}{\tau_o} - \frac{1}{\tau_p}\right)^3$$

The digital computer thereby linearizes the transducer output, producing a binary representation of the actual pressure. This process can be done with extreme precision and will not degrade the inherent accuracy of the transducer. The overall accuracy of this operation can be as good as 0.0128% of full scale. Furthermore, once the computer is available, it can be used to convert the binary format to BCD for use with a decimal digit readout. More will be said about the computer and its capabilities later.

There is a large family of pressure measuring applications that does not need and cannot use the digital output discussed above. The process control business, for example, is one that is presently built around the use of analog devices primarily because of the unavailability of rugged digital devices. However, analog systems could benefit from the inherent accuracy or the stability of a digital transducer. Having the transducer period as a binary number, it is easy to convert this digital output to analog by many of various proven methods. One, which has been popular, is the inexpensive scheme shown in Figure 6. The precision of the analog conversion of this circuit is a function of the resistors used. If they are carefully selected for value and they are of a quality to preclude thermal problems, the conversion should be fairly good. Since the basic transducer output is about 5% non-linear, the analog output cannot be this good. Although this non-linearity probably is not good enough for use in most test instrument applications, it is quite acceptable for

closed loop analog control systems which are insensitive to slight non-linearities but which can benefit tremendously from the stability exhibited by the digital transducer. This would satisfy the requirement of many process plants for a transducer that can be installed and "forgotten".

Another option is available which yields a linear analog output for those test instrument setups and certain complex control systems requiring a highly linearized output voltage. For this situation, the frequency output of the computer is first converted to a binary representation of period, as discussed above. The conversion from binary period to linear analog is done by analog computer and comparator techniques — a process that yields a 0-5 VDC output, linear to within ±0.002 volts. The overall transducer accuracy, including such things as calibration, repeatability, resolution, long term stability, ambient temperature, and linearity, is approximately ± 0.04% of full scale. This accuracy attests to the desireability of using the digital transducer as the "front-end" of an analog system.

COMPUTER

When the digital computer is used with the pressure transducer for linearization and temperature compensation, its basic job is to take the binary representation of transducer period, averaged over some value such as 64 transducer cycles, combine it with the calibration constants of the transducer pressure sensing element, and compute the value of pressure. This computation involves solving the third order polynominal equation given previously. The computer also may have the job of compensating the pressure output for ambient temperature effects of the gas being measured. In this case, assuming that the transducer is not of the self-heated variety, the compensation can be done from a 3-segmented curve representing ΔT as a function of ambient-temperature.

The computer is a compact assembly of three TO-8 cans and five 1-1/4 x 1-1/4 inch flat pack hybrid circuits. These components are fabricated by interconnecting medium scale integrated (MSI) circuit devices together in a multi-layer, three dimensional layout resulting in high density packaging.

The foundation for each of the subassemblies is an alumina or beryllia substrate upon which conductive gold circuit and crystallizable dielectric patterns are screened and fired to form a solid multi-layer circuit. The MSI component devices are then bonded to the substrate. Interconnections between MSI devices and substrate circuit patterns are made with fine gold lead wires which are attached by thermocompression bonding. Figure 7 is a 8X magnification photograph of a TO-8 can hybrid circuit showing the MSI devices attached to a .350 x .350 inch alumina substrate. Figure 8 is a 5X magnification of a typical flat pack assembly. The five large devices in Figure 8 are ceramic capacitors, the small black devices with three lines showing are resistors, and there are three MSI circuits.

There are several reasons for using hybrid construction of this type for the computer electronics. First, hybrid circuits are flexible and changes can be made to expand the computer and meet customer requirements without incurring great cost. Second, this form of multi-layer hybrid construction results in a mechanical structure that is, indeed, rugged and able to take vibration and shock loads without failure. Third, the subassembly is repairable and can be salvaged if a bad device is found during post-production acceptance testing. And finally, the assembly is small which permits compact packaging.

ACCURACY AND STABILITY

We might concede that the vibrating cylinder is an interesting and an unusual concept for measuring pressure, but why is it necessarily better than other vibrating element or well known analog types? The answer to this is many faceted, as we shall see.

Damping - The vibrating cylinder pressure transducer has many attributes which enhance its position among transducers. One of the most important characteristics inherent in the design is the transducer's response to vibratory excitation at its natural frequency. All mechanical structures have some damping. This damping represents lost energy which must be added by an external, vibratory driving force. Ideally, the excitation force vector and the vibrating cylinder displacement vector should be exactly 90° out-of-phase at the resonant operating condition. Certain factors such as temperature effect, circuit loading, magnetic coupling, and operating frequency cause this phase relationship to change. The presence of system damping and this phase change causes the drive coil to operate slightly off resonance. This, of course, produces a direct error in the frequency-to-pressure relationship. However, if the system damping is low enough, the effect of system phase change will be small.

A vibrating device with low damping also has a "sharp" or narrow resonance response curve. One way to express the sharpness of the resonance curve is to measure the amount of energy lost or dissipated per cycle relative to the energy stored in the structure per cycle. At resonance, the stored energy is equal to the kinetic energy at maximum velocity (zero axis crossing) or the potential energy (at maximum amplitude). The energy ratio is denoted by the letter "Q" and represents a figure of merit with regard to the absence of system damping.

$$Q = \frac{\text{Average energy stored per cycle}}{\text{Energy dissipated by damping per cycle}} .$$

It is evident that when damping is low, the Q will be high. A convenient method of obtaining this figure of merit is to consider the actual amplitude response curve of the mechanical structure. Let the maximum amplitude of vibration at resonance be denoted by G_n, see Figure 9. Also, let an amplitude of G_n be denoted by H. If the resonant amplitude G_n occurs at a frequency f_n and the frequencies accompanying the amplitude H are f_1 and f_2, where $f_1 < f_n < f_2$, the value of Q is expressed by

$$Q = \frac{f_n}{f_2 - f_1} .$$

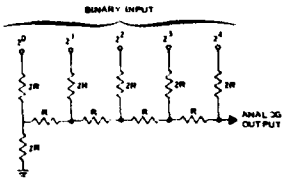

INPUT REGISTER POSITION						ANALOG OUTPUT VOLTAGE WHERE LOGIC "1" = V_{IN} = 5 V (TTL)
	2^4	2^3	2^2	2^1	2^0	
BINARY NUMBERS	1	0	0	0	0	1/2 V_{IN} = 2.5 V
	0	1	0	0	0	1/4 V_{IN} = 1.25 V
	0	0	1	0	0	1/8 V_{IN} = 0.625 V
	0	0	0	1	0	1/16 V_{IN} = 0.3125 V
	0	0	0	0	1	1/32 V_{IN} = 0.15625 V
	0	0	0	0	0	0 V_{IN} = 0.0
	1	1	1	:	1	(1/2 + 1/4 + 1/8 + 1/16 + 1/32) V_{IN} = 4.84375 V

FIGURE 6. DIGITAL TO ANALOG CONVERSION

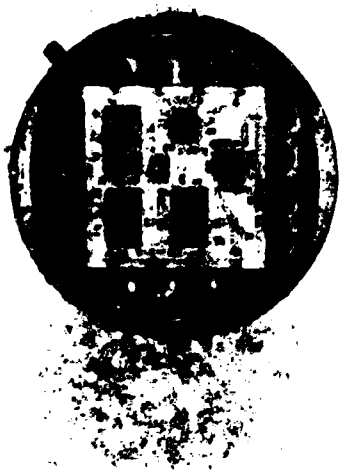

FIGURE 7. 8 X MAGNIFICATION PHOTOGRAPH OF HYBRID CIRCUIT IN TO-8 CAN

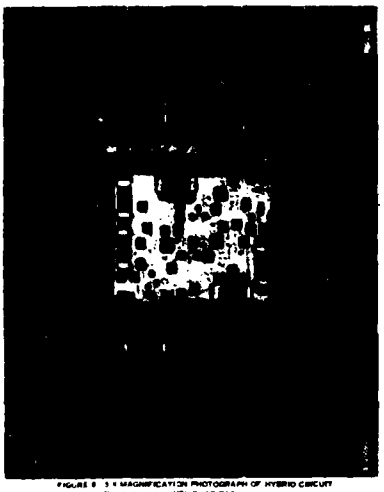

FIGURE 8. 5 X MAGNIFICATION PHOTOGRAPH OF HYBRID CIRCUIT IN 1-1/4 X 1-1/4 INCH FLAT PACK

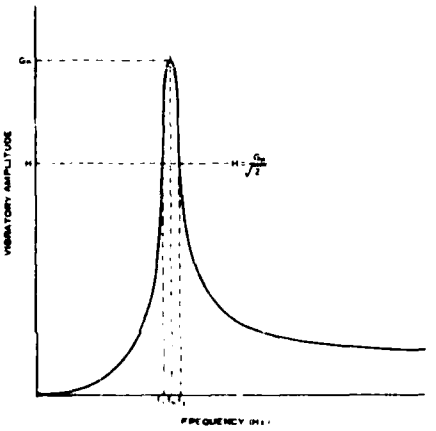

FIGURE 9. VIBRATING CYLINDER FREQUENCY RESPONSE

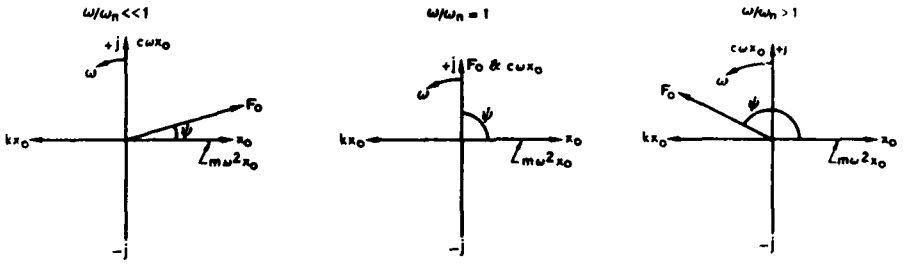

EQUATION OF MOTION: $m\ddot{x} + c\dot{x} + kx = F(t)$

ASSUME SOLUTION $x = x_0 \sin \omega T$

ASSUME MAJOR EXCITATION $F(t) = F_0 \sin \omega T$

EQUATION BECOMES $-m\omega^2 x_0 \sin \omega T + cx_0 \cos \omega T + kx_0 \sin \omega T = F_0(t)$

FIGURE 10. VECTOR RELATIONSHIPS

The Q of the vibrating cylinder pressure transducer is above 5000, which means that the resonance curve is only one Hz wide at a natural frequency (f_n) of 5000 Hz. This represents very low damping.

Perhaps in a more classic solution, we can assume a single-degree-of-freedom system and express the damping as a force in the differential equation of motion

$$m\ddot{x} + c\dot{x} + kx = F(t) \quad .$$

The damping force is $F_d = c\dot{x}$, where c is the damping constant and $\dot{x}$ is the vibratory velocity. The damping factor is defined by the ratio $\zeta = c/c_c$, where $c_c = 2m\omega_n$, m = equivalent mass, and ω_n is the circular resonant frequency. We can write an expression for the ratio of the actual vibratory amplitude to the static deflection. This ratio is the magnification factor of the mechanical structure, expressed in terms of the damping factor and the circular frequency ratio ω/ω_n, ie,

$$MF = \frac{x}{x_{static}} = \frac{1}{\sqrt{\left[1-\left(\omega/\omega_n\right)^2\right]^2 + \left[2\zeta\,\omega/\omega_n\right]^2}} \quad .$$

The maximum vibratory amplitude ratio, or magnification factor, occurs at $\omega/\omega_n = \sqrt{1-2\zeta^2} < 1$, and yields

$$MF_{max} = \frac{x_{max.}}{x_{static}} = \frac{1}{2\zeta\sqrt{1-\zeta^2}} \quad .$$

If the ratio of these magnification factors is taken, we obtain

$$\frac{x}{x_{max.}} = \frac{2\zeta\sqrt{1-\zeta^2}}{\sqrt{\left[1-\left(\omega/\omega_n\right)^2\right]^2 + \left[2\zeta\,\omega/\omega_n\right]^2}} \quad ,$$

and this equation can be used to determine the mechanical damping factor by knowing that at $x/x_{max} = 1/\sqrt{2}$, $\omega/\omega_n = \frac{4999.5}{5000.0}$. The damping factor computes to $\zeta = 0.0001$. To show the significance of this, consider the angular relationship of the vector forces involved. Referring to Figure 10, we can draw the force vectors and compute

$$\tan\psi = \frac{c\dot{x}}{kx - m\ddot{x}} = \frac{c\omega}{k - m\omega^2} = \frac{2\zeta\,\omega/\omega_n}{1-\omega/\omega_n^2} \quad .$$

A plot of this relationship is shown in Figure 11. It is evident that when the damping factor ζ is small, the effect of ψ upon the frequency of vibration is minimized. That is, if the driving circuit force cannot be maintained at exactly 90° with respect to the vibratory motion vector of the pressure transducer inner cylinder, it is advantageous to have as little damping as possible to avoid large error in frequency.

In order to evaluate the actual effect that damping or Q has upon the transducer's output frequency, a computation has been made using the equations discussed above. Many solid mechanical structures have Q's of the order of 50 and lower. This represents a damping factor of 1% or higher. The Hamilton Standard vibrating cylinder pressure transducer has a Q above 5000. Figure 12 is a plot showing the percent error in output frequency as a function of Q and the variation in the phase relationship ψ. These curves show that a phase variation of $\pm 10°$ can produce almost an order of magnitude larger error in frequency than one of $\pm 10°$. Observe also that the Hamilton Standard design has a maximum phase error of $\pm 10°$ which produces a frequency error of only $\pm 0.00176\%$ compared with a theoretical Q = 50 device which would have an error of $\pm 0.1227\%$ for the same $\Delta\psi$.

Thus, we have established the major advantage of having a high Q vibrating transducer — namely, to make the instrument insensitive to small phase changes in the drive control loop.

Repeatability and Hysteresis - Another attribute of the vibrating cylinder pressure transducer that makes it an outstanding design is its low hysteresis and excellent repeatability. Repeatability is a measure of the maximum deviation from the average of corresponding data points taken from repeated tests under static and identical conditions for any one pressure value. The non-repeatability of a transducer is most often the result of drift and hysteresis due to strain of the sensing element, friction in pivot points, the creep of adhesives, etc. The vibrating cylinder transducer has none of these problems. Since there are no moving parts such as bellows or balance beams, the device is not susceptible to coulomb friction. The vibrating inner cylinder is welded to the heavy base ring of the protective outer cylinder, and this subassembly is clamped to the transducer base so that no relative motion can exist. If there should exist some tendency for an interjoint or intergrannular coulomb effect, this hysteresis source is removed by the vibration inherent in the transducer.

The vibrating cylinder undergoes a static stress proportional to pressure. In a closed-end cylinder these stresses are tensile, compressive, shearing and bending. Nonetheless, several things are apparent. As long as the material is stressed below its elastic limit, there will be no short term tendency for any permanent deformation. Second, if the stresses are well under the endurance limit of the material, the cylinder will not exhibit a degradation due to fatigue. Another factor, perhaps less apparent than the others but which can effect the hysteresis and repeatability of the transducer, is stress creep. Stress creep occurs as a three stage phenomenon which is a function of stress, temperature and time. For the materials of construction of the vibrating cylinder, a normal operating temperature of less than 250°F, and a normal maximum working stress level of only 6% of the yield, the effects of stress creep are negligible. Hence, we say the effect of all of the above factors is better than $\pm 0.0001\%$ of the full scale pressure being measured by the transducer.

Long Term Stability - A third attribute of this transducer is its long term stability. Stability is a measure of the transducer's freedom from changes in performance due to internal causes over a period of time. The long term referred to is a period of one year. Certainly the user has every right to expect a precision device to maintain its calibration for some period of time, and all too often that time span is measured in days. As has been discussed above, the vibrating cylinder has no moving parts, no tomed joints, and very conservative stressing — exactly what is expected of a precision instrument. The one year long term stability of the vibrating cylinder pressure transducer has been determined by tests to have a 2σ level of $\pm$ 0.0060% F.S. Although this is a very low number, we may ask what causes it. The investigation of many parameters has led to the conclusion that this small degradation in performance in the long term is due to the porosity of (1) the electron beam welded joints that seal the reference vacuum (approximately 10^{-5} torr) between the inner and outer cylinders and/or (2) the micro-porosity of materials used in fabricating the instrument. This pressure change is representative, in standard metric form, of a leak rate of 1.45×10^{-12} Torr liters/sec. This rate of leakage is the same order of magnitude as the degassing rate of steel. Although it has not been proven conclusively, the degassing of the cylinder assembly walls and welds is presently thought to be the origin of the long term stability values measured.

Resolution - The resolution of the basic vibrating cylinder pressure transducer is infinite. Frequency of the transducer varies with pressure changes in accordance with a mathematical expression reflecting the laws of elasticity and conservation of energy. There is no granularity to this measurement.

Resolution does become a part of the discussion, however, when the basic frequency signal is converted accurately to an analog or pure digital (binary or decimal) format. As explained above in the section under Output Considerations, most of these techniques involve a frequency sampling time and perhaps a linearizing computation time. Consider the conversion from frequency to the binary representation of period. The resolution is determined from the relationship

$$\frac{1}{N_{\ell}} = \frac{1}{(\tau_o - \tau_p)\, f_{\ell} N_t}$$

where N_{ℓ} = accumulated clock cycle count (cycles)

N_t = transducer cycle count (cycles)

f_{ℓ} = clock frequency (Hz)

τ_o = $1/f_o$, the transducer period at zero pressure (sec.)

τ_p = $1/f_p$, the transducer period at the measured pressure, P. (sec.)

The practical upper limit of the clock frequency is 15 megahertz. Frequencies higher than that begin to produce crosstalk and problems in mechanical packaging. Typical values for the transducer period at zero pressure and say 20 psia are $1/f_o$ = 1/4500 Hz or τ_o = 222.2 microseconds and $1/f_{20}$ = 1/5500 Hz or τ_{20} = 181.8 microseconds. The value of N_t is somewhat arbitrary and depends upon the application. For measurements where fast response is required, the period sampling time must be shortened as required to meet the need. For the benign laboratory environment, the sample taken can be very large. In general, however, it is convenient to sample on the basis of a power of 2 since the conversion circuitry generally uses binary logic elements. For this example, consider the use of a seven bit counter such that the sampling time ends just as the seventh bit changes from 0 to 1. Thus, the trigger count is the change from a decimal count of 63 = $0111111_{(2)}$ to a decimal count of 64 = $1000000_{(2)}$. Substituting back into the above equation yields a resolution of

$$\frac{1}{N_{\ell}} = \pm \frac{1}{\{222.2 - 181.8\}10^{-6} \cdot 15 \cdot 10^{6} \cdot 64} = \pm \frac{1}{38784}$$

$$= \pm 0.00258\%$$

Linearity and Calibration - The calibration of the instrument is the process of determining the constants A, B, and C in the equation

$$P = A(f_o - f_p) + B(f_o - f_p)^2 + C(f_o - f_p)^3$$

This third order equation is a good approximation of the relationship between pressure and frequency. It has been found that higher order equations make very small improvements in accuracy. The coefficients A, B, and C could be determined by calibrating the transducer at three points and then solving simultaneously the three equations that result. This technique would not allow the error of the determination to be established since no redundant data is used. A better method is to calibrate the transducer using several times the minimum amount of data required, usually 10 points. This data is then used in a computerized curve-fitting routine which fits the 10 calibration points to a third order curve and calculates the absolute deviation from that curve. This deviation is what is meant by the end-point linearity, and on this basis it is found that the end-point linearity of the transducer is $\pm$0.0080% of full scale.

The calibration of high accuracy transducers is a difficult problem. It is difficult to determine that the calibration device is as good or better than that which is being calibrated. The dead-weight tester is about as consistent and trouble-free a device as is practical to use, and it can be calibrated and certified by the National Bureau of Standards.

The calibration errors have been budgeted in three categories. The first error is associated with the weights used in the calibration process. The weights are placed on the tester pan which is supported by a piston in a cylinder. This assembly closes a volume

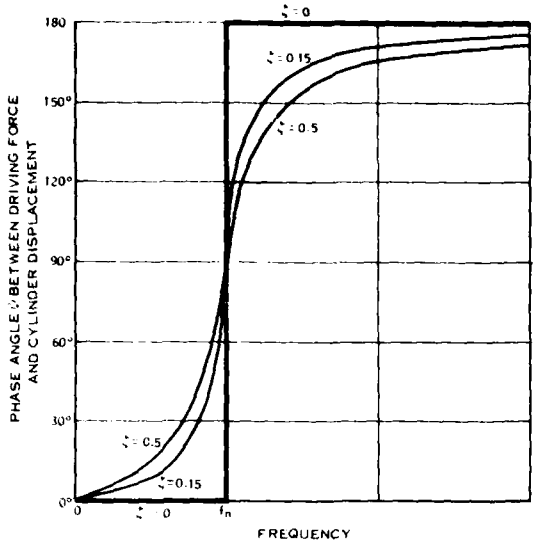

FIGURE 11. PHASE ANGLE BETWEEN FORCE AND DISPLACEMENT VECTORS AS A FUNCTION OF FREQUENCY AND DAMPING

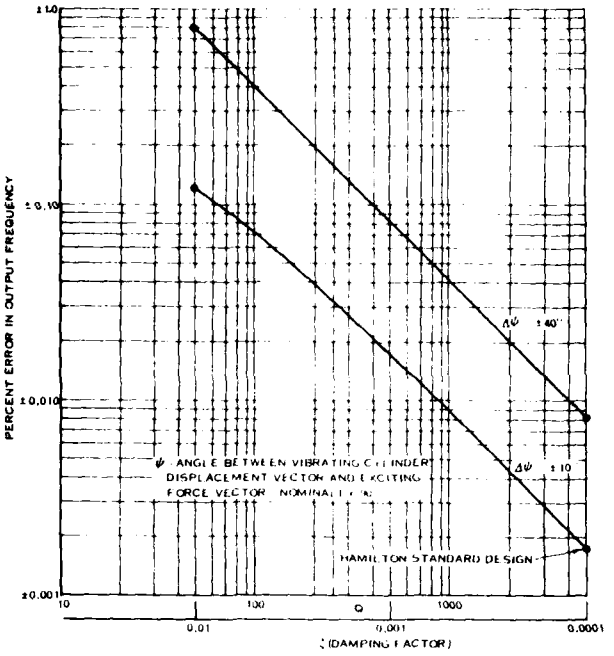

FIGURE 12. TRANSDUCER FREQUENCY ERROR AS A FUNCTION OF Q AND Δψ

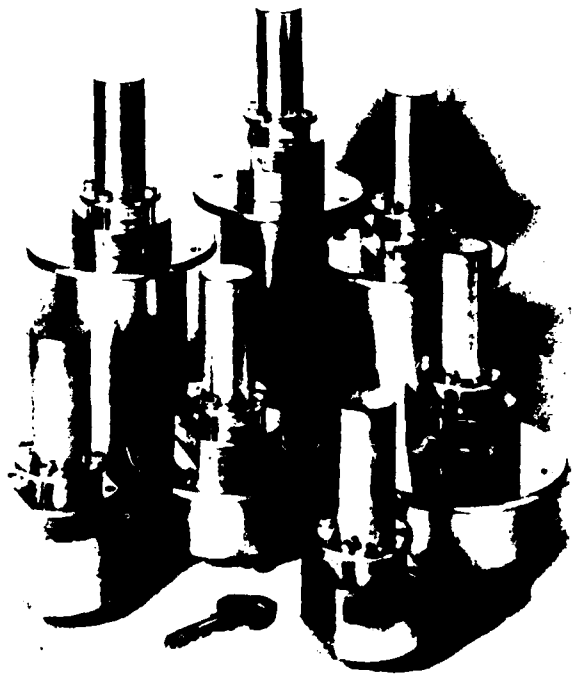

FIGURE 13. PRESSURE TRANSDUCER MODELS

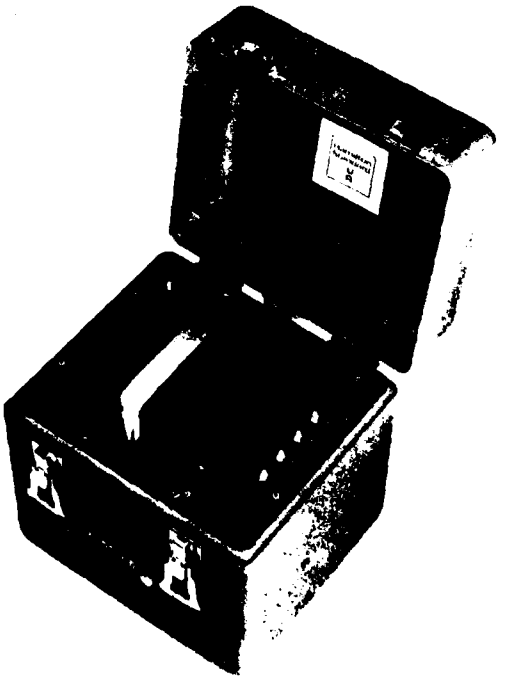

FIGURE 14. PORTABLE PRESSURE TRANSDUCER

that is connected by plumbing to the transducer. The weights load the piston, and this load, applied over the piston/cylinder area, creates a gas pressure in the closed volume. The weights are certified by the National Bureau of Standards (NBS) and represent a ± 0.0050% of point calibration pressure error.

The second error is in conjunction with the area of the piston/cylinder assembly. This is also calibrated by the NBS, and the error in area represents a calibration pressure error of ±0.0045% of point.

The third category of error in the calibration process represents a number of factors which together and by practical experience over years of laboratory calibration service amount to an error of ±0.0005 psi. The factors included in this category are:

(a) Friction between piston and cylinder of the dead-weight tester.

(b) Level of weight pan.

(c) Unbalance of the weights on pan.

(d) Deflection of cylinder side walls under pressure.

(e) Piston temperature.

(f) Value of "g" acceleration at the calibration site.

(g) Residual air pressure in bell jar covering tester.

The total calibration error is represented by the expression

Calibration Error = $\pm\{[(.00005)\,\text{Pressure}]^2 + [(.000047)\,\text{Pressure}]^2 + [.0005]^2\}^{1/2}$ psi and computes to ± 0.0073% at 20 psia.

Density - The vibrating cylinder pressure transducer's natural frequency is a function of the equivalent mass of the vibrating system. The vibrating system includes not only the metal walls of the inner cylinder but also the mass loading of the gas in contact with it. The vibrating cylinder pressure transducer is designed for measuring gas pressure, not liquids. When the gas is in contact with the vibrating cylinder walls, it is "pumped" back and forth between antinodes, and because of gas density effects, the gas adds an effective mass to the cylinder. Ordinarily this causes no problem because for any given gas the pressure - density relationship is constant if the temperature is constant. Therefore, the effect of density is removed during the calibration process for a given gas.

Temperature - Temperature affects both the elastic constant of the vibrating cylinder and the density of the gas in contact with the cylinder. Fortunately, the frequency of the vibrating cylinder is proportional to the square root of the elastic constant and inversely proportional to the square root of the density. These charateristics tend to be cancelling. If the transducer is left uncompensated, the pressure error due to temperature is an off-set linear relationship such as the following for a 20 psia unit:

$$\text{Error} = \pm\,[0.000232P + .00035]\ \%/^{\circ}F.$$

If the user compensates for temperature changes by means of a signal from a diode temperature sensor affixed to the spool body, it is reasonable to assume that this compensation can be accomplished to within ±1.0°F, and then the above equation is applied on an absolute basis. The error of 20 psia would be ±0.005% of point.

Perhaps a better method of temperature compensation is achieved by building a heating coil into the spool body and controlling the temperature of the internal structure and gas by means of a simple, proportional, closed loop control. A bridge circuit is used to set the control reference, and this reference is independent of power supply variations. The error voltage established by the difference between the sensed temperature and the reference is amplified and used to control the rectified heater power voltage. This set point is normally placed at 160°F, a temperature high enough to eliminate condensation problems. Under these circumstances, the absolute pressure error equation for the 20 psia transducer will be

$$\text{Error} = \pm\,[0.0000465P + .00007]\ \%$$

which, at 20 psia, computes to ±0.001% of point.

Vibration - As explained previously, the inner cylinder vibrates in a symmetrical, four lobed hoop mode. Hence the effect of external lateral vibration on the driver or pickup elements of the transducer cancels out. The structure is stiff enough to be free of lateral resonances below 2000 Hz. Above 2000 Hz, one begins to find some cantilever bending modes of the spool body and the cylinder assembly. Even at these lateral modes of vibration, the error is random and tends to average out if the transducer sampling time is long enough.

There is no error due to axial excitation.

Error Summation - The error sources discussed above represent all of the significant factors that determine the overall accuracy of the vibrating cylinder pressure transducer concept. The errors are all random, which means that there is an equal chance for the error to be either positive or negative. Some of the errors are inherently percent-of-point based while others are percent-of-full scale based. Errors are not necessarily statistically distributed in the same manner (i.e., Gaussian, Weibull, rectangular, etc.) however, they must all have the same multiple of standard deviation, i.e., all σ , or all 2σ , or all $n\sigma$, and not a mixture.

Then according to the "Central Limit Theorem", no matter what the distribution of independent variables (square, rectangular, Gaussian, Weibull skewed, or other) as a limit they approach the root-sum-square of a Gaussian distribution. Hence, the importance of the Gaussian distribution in the determination of error.

In order to obtain the total error for a given pressure transducer, certain assumptions have been made as follows:

(a) The transducer is temperature controlled.

(b) A digital computer is used to linearize the pressure transducer's numerical output.

(c) A transducer cycle sample count of 64 is used in conjunction with a 15 MHz precision clock.

(d) The pressure transducer has a full scale value of 20 psia.

We can combine all of 2σ errors in the statistical manner outlined above to yield the results shown below:

Damping	$\pm 0.0018\%$
Calibration	$\pm\{(.00100)^2+(.00094)^2+(.0005)^2\}^{1/2} \cdot 100/20 = \pm 0.0073\%$
Linearity	$\pm 0.0080\%$
Repeatability	$\pm 0.0001\%$
Resolution	$\pm 0.0026\%$
Long Term Stability	$\pm 0.0060\%$
Ambient Temperature	$\pm 0.0010\%$

$$\% \text{ Error at 20 psia} = \pm\{(.0018)^2+(.0073)^2+(.0080)^2+(.0001)^2+(.0026)^2+(.0060)^2+(.0010)^2\}^{1/2} \ldots \pm .0128\%$$

PACKAGING

The packaging philosophy for all of the transducer models, from the basic model to that with a linearizing digital computer, features the incorporation of all hardware into one, self contained module for convenience of use. A family of these transducers is shown in Figure 13. As all transducer manufacturer have found, each user is different, has an unusual application, and requires a somewhat different output format, counting resolution, shape, size, etc. Hence, the component subassemblies are designed to be conveniently separated or varied as required by the users.

APPLICATIONS

The applications for pressure transducers are many and varied. Some require the best transducer available in order to achieve the desired result. The vibrating cylinder pressure transducer is being used or proposed for many applications in process control, laboratory analysis, test instrumentation and complex control systems. Some of these are the

(a) measurement of very high altitude flight characteristics of aircraft

(b) flow measurement of natural gas in pipeline systems

(c) measurement of cooking and flow pressures in food processing

(d) measurement of pressure in diesel engines for diagnostic purposes

(e) measurement of pressure with micro-pressure resolution for laboratory analysis

(f) measurement of the pressure ratio across an aircraft engine for flight control

(g) measurement of air speed

It is applications such as these that led to the development of the vibrating cylinder pressure transducer, so it is appropriate to discuss two demanding applications that have benefitted by the use of this instrument.

NUCLEAR POWER STATIONS

As our resources are expended at an ever increasing rate, managers of electric power companies are under more pressure to find better ways of serving the public and industry without producing by-products which contaminate the environment. All this must be done for a reasonable cost. A strong trend toward the use of nuclear reactor power stations has been evident during the last two decades. New nuclear electric generating stations are being built and more are in the planning and design stage. Along with this growing population of operating plants, we find new safety regulations being written with which to control this infant industry. One standard, ANS 7.60, written by the American Nuclear Society, relates to the subject of pressure transducers. It requires that leakage from the containment structure surrounding the nuclear reactor be monitored. This requirement has been echoed and augmented by the AEC in the proposed regulation (Federal Register, Vol. 36, No. 167 - Friday, August 27, 1971) relative to leakage testing requirements for the primary reactor containment, the seals and gaskets associated with elements penetrating the primary containment, and containment isolation valves. These regulations require periodic tests to be made on the structure to determine leakage or leakage potential which, in an emergency, might accidentally release radio-active materials into the atmosphere that could endanger the public health and safety.

Several tests are proposed. One is the Type A test used to verify the leakage of the reactor containment when the unit is first constructed and later on at periodic intervals. A positive pressure is applied to the reactor building and pressure data is taken on an hourly basis over not less than 24 hours. These leakage data are fitted to a linear least-square curve as a regression problem in statistics. This leakage must fall within the licence specifications for the individual and specific power generator under investigation. Thereafter, three Type A leakage tests are made within the span of ten service years. Several variations of this test are permitted; however, the intent of them all is the same - to verify the integrity of the reactor containment.

Type B and Type C tests are done on the seals and gaskets, and the isolation valves, respectively. These leakage tests are conducted at each major refueling of the reactor, but not longer than at two year intervals. Here again variations in this requirement exist, depending upon the type of equipment.

The above tests call for pressurizing the containment structure which can be a building, a vessel, or an undeground housing for the components of the reactor system. These components include the primary containment vessel, penetrations of this vessel, and associated valves. The pressures for testing are either the peak containment internal pressure expected as a result of a hypothetical loss of reactor coolant, or a reduced pressure of not less than 50% of the peak pressure.

The method of leak detection is to measure the rate of decay of the absolute internal pressure for 24 hours at one hour intervals. The resulting leakage for each interval is calculated from the expression

$$\% \text{ Leakage/Hour} = \left[1 - \frac{T_1 P_2}{T_2 P_1}\right] 100,$$

where T and P are the measured temperatures and pressures at the beginning (1) and end (2) of the interval. These results are used in a least-squares statistical calculation of the 24 hour leakage rate. Differentiating the above equation, a statistical expression for the error in the leakage determination is obtained to be

$$\Delta(\% \text{ Leakage/Hour}) = \left\{\left(\% \frac{\Delta P_1}{P_1}\right)^2 + \left(\% \frac{\Delta P_2}{P_2}\right)^2 + \left(\% \frac{\Delta T_1}{T_1}\right)^2 + \left(\% \frac{\Delta T_2}{T_2}\right)^2\right\}^{\frac{1}{2}}.$$

If the testing is done under well controlled, constant temperature conditions, the temperature error terms can be disregarded, leaving only the pressure measurement error. Since leakage is small, pressure changes over a one hour span are also small, and, therefore, calibration and long term stability errors can be neglected. The major error sources are repeatability and resolution. Since the repeatability of the vibrating cylinder pressure transducer is better than $\pm 0.0001\%$ of full scale, the error in leakage determination resolves to one of transducer resolution. The resolution of the vibrating cylinder pressure transducer is inherently infinite. When converting from frequency to binary period, the resolution can be any desired level depending only upon the sampling time of transducer cycles and the precision clock frequency.

Another measurement made by the subject transducer in the nuclear power-generating station is that of ventilation system pressure. Some of the structures used in the power plant complex have ventilation systems that operate at a few inches of water less than atmospheric pressure. This assures that leakage of the structure will be negative. The outflow from the ventilating system is passed through filters where contaminants are removed. These contaminants could be radioactive, so they are disposed in a manner controlled by the Atomic Energy Commission. The pressure balancing of the pressure duct system of vents is important so that proper ventilation flow is established without recirculation of potentially contaminating particles. The pressure balancing of these ventilation ducts is done more accurately using a portable vibrating cylinder pressure transducer because of its stability and resolution. A photograph of this portable device is shown in Figure 14.

Aircraft Air Inlet Controls

As aircraft flight speeds become faster and faster, the role of the air induction system, or air inlet control, for the jet engine becomes more and more important. This is a natural consequence of the increased ram compression available at supersonic flight speeds. Even at moderate supersonic Mach numbers the amount of ram compression available exceeds that of the jet engine compressor; hence, the inlet becomes an important part of the engine cycle and the efficiency of the propulsion system is closely coupled with the efficiency of the air inlet system. The primary function of the supersonic inlet is to efficiently convert the kinetic energy of the inlet air to pressure; but, in addition, the inlet must supply the correct amount of air at velocities and pressures which the engine can accept, and it should do this with low drag due to spillage of excess air over the entire range of aircraft operation. With increasing flight Mach number, the task of the inlet becomes more difficult, and the inlet must be more sophisticated to meet the wide range of requirements. The inlet control senses the inlet/aircraft operating conditions and, using the high speed computation of a digital computer, modifies the inlet geometry by adjusting the inlet ramp position and by-pass door opening to control inlet capture area, shock wave pattern, and airflow spillage. These elements are shown in Figure 15.

High speed aircraft are usually operated at predetermined Mach numbers instead of specific airspeeds. Mach number is the ratio of the speed of an object to the speed of sound in the same medium and at the same temperature. Sonic velocity and Mach number vary with air temperature, therefore, at standard day conditions, the air speed which corresponds to a given Mach number will vary with changes in altitude.

In the case of an aircraft which is designed to fly at speeds of Mach 2.0 and greater, the air velocities which are encountered at the inlet duct are much higher than the engine can efficiently use. The air inlet, its geometry changing mechanism and control, provides the means to slow this air. This process of slowing incoming air results in a static pressure rise, or compression, and the amount of compression is determined by the kinetic energy of the air stream flowing past the aircraft. On a subsonic jet aircraft, the engine compressor inlet pressure is about 1.8 times the free stream static pressure at a cruise Mach number of 0.95. This compression ratio increases to approximately 17 at a Mach number of 2.5. The importance of inlet performance at high Mach conditions is evident when this duct pressure ratio of 17 is compared with typical engine compression ratios of 15-25. As the duct pressure ratio increases, complex variable geometry duct designs are required, along with intricate control systems, to achieve high efficiency.

The kinetic energy of a supersonic flow stream is converted to pressure by passing the flow through a convergent-divergent passage. The flow will be supersonic but decreasing in Mach number in the convergent section of the passage, and a transition to subsonic flow will occur at the throat of the passage where the air passes through a normal shock wave. At this point, the flow velocity will have been reduced to approximately 0.8 Mach number. The flow stream then passes through a divergent passage where the velocity can be reduced as low as is required by expanding the divergent passage to a larger and larger cross-sectional area. In this compression process, lowering the upstream Mach number requires more and more contraction of the passage at the throat in order to efficiently decelerate the flow stream to a velocity slightly above Mach 1.0 before passing through the normal shock wave.

A system of bypass doors is under the supervision of the air inlet control to reroute the air that the engine cannot efficiently handle. By-pass of this air internally assures a minimum drag penalty to the aircraft because of minimum inlet air spillage, permits the enterance of air at the engine compressor face to be at the correct pressure, and helps to position and stabilize the normal shock at the inlet throat.

Although many types of measurements are required by the inlet control such as temperature, displacement, vibration and hydraulic pressure, the most difficult parameter to measure accurately is pneumatic pressure. This is because of the large range of pressure to be measured and the associated large turn-down ratio (maximum to minimum pressure ratio). The turn-down ratio often approaches 20 to 30 to 1 which makes the selection of pressure transducers difficult since accurate measurements must be made at both ends of the range of pressures. The accuracy of the pressure measurement device is extremely critical as is the computation of local Mach pressure ratio because any error in sensing or calculating results in off-design inlet operation. The signals received from the airplane pitot-static system, P_{To} and P_{So}, provide the means to compute local Mach pressure ratio. The ratio of P_{To} to P_{So} provides a unique signal which is used to schedule ramp position. Pressures P_{To} and P_{So} are transduced by vibrating cylinder pressure sensors. The ratio of these signals is calculated by a digital computer.

Bypass door control is based on an aerodynamically closed loop principle of operation. Pitot-static pressure sensing probes are located in the engine inlet duct, downstream of the normal shock. The probe location is selected so that the desired throat pressure ratio can be maintained, over the range of automatic operation, at a fixed or nearly fixed ratio of signal pressures, $(P_T/P_S)t$. Pressures P_{Tt} and P_{St} are also sensed by vibrating cylinder pressure transducers, and the pressure ratio is determined by the digital computer.

Of the four vibrating cylinder pressure transducers used to measure local Mach pressure ratio and throat pressure ratio, there are three high pressure sensors and one low pressure sensor, each sensor being a separate sub-assembly. The four pressure transducers produce variable frequency output signals of 5 volts peak-to-peak amplitude. The P_{So} transducer output ranges from 4.2 KHz to 5.5 KHz while the other three transducers range from 5.4 KHz to 7 KHz. The transducer electronics are assembled on three small printed circuit cards. One board contains the driver amplifier circuit for the vibrating cylinder. The second card accepts the output from a temperature sensitive diode located on the transducer spool body, amplifies it, and feeds it to a transducer multiplex network which interrogates each transducer temperature for compensation by the digital computer. The third card contains a read only-memory which stores the calibration constants for the transducer. This memory is interrogated by the multiplexer part of the digital computer program control. A photograph of this subassembly is shown in Figure 16 and 17.

A special purpose digital computer performs all computation, scheduling and decision making functions required in the operation of the air inlet control. The computer processor receives the four pressure transducer signals as 16 bit binary numbers. It also uses information on total temperature, angle of attack, and ramp and bypass door position. The major outputs of the processor are the position command signals to the ramp and bypass door servo valves, each of which is updated about 88 times per second. These signals are converted to an analog format and delivered to electrohydraulic servo valves through 10 bit D/A converters, one for each actuator.

All pneumatic pressure measurements require fast response rates because of transients introduced by aircraft attitude variations. Transducers of the type generally used for laboratory or wind tunnel measurements do not usually have suitable transient response for flight. During flight, the aircraft accelerates and climbs to cruise altitude in an unscheduled manner which precludes stabilizing on a given flight condition for any significant time period. Also, variations of in-flow angle to the inlet are induced by pitch and yaw of the airframe. Therefore, transient measurements must be made with instrument response that is flat to 15 cps. This means that the installation of the pressure transducer must be made so as to keep its distance from the sensing probe to a minimum. One of the major deterrents to fast response frequency is the use of long pneumatic hookup tubes. Fast response also means that the transducer cycle count during the conversion from frequency to binary period must be minimized. The combination of these parameters in the design of a responsive air inlet control is a delicate task.

The design of air inlet control systems has always been difficult and complex. In the latest high performance, high Mach number aircraft, this task would be all but impossible were it not for the accuracy and stability of the vibrating cylinder pressure transducer. An exploded view of an electronic air inlet control is shown in Figure 18. The assembled unit is shown in Figure 19.

CONCLUSIONS

The Hamilton Standard vibrating cylinder digital pressure transducer is truly a unique device — not only because of its unusual configuration and operating principles but also because of its uncommon combination of accuracy, stability, small size, and ruggedness. The idea of a vibrating device to sense pressure is not new. Many devices comprised of vibrating wires, vibrating tuning forks, vibrating diaphragms, etc. have been conceived and built. However, none of these configurations have the stability and high Q of the vibrating cylinder pressure transducer.

The vibrating cylinder natural frequency changes with the pressure being measured. The basic transducer produces a square wave, variable frequency output signal. This signal, although about 5% non-linear, can be used as a frequency proportional to pressure, as a binary digital number representing transducer

period which is inversely proportional to pressure, or as an analog representation of the frequency which again is proportional to pressure. Any of these outputs have the inherent high stability and low hysteresis of the basic transducer. The latter two represent conversions which, if done carefully and with resolution considered, can yield output signals of the highest accuracy. There are numerous applications which require that the pressure transducer have a linear output. In those instances, the vibrating cylinder pressure transducer includes a digital computer if a linearized digital output is desired, or an analog computer and comparator if a linear analog signal is needed. For either of these instruments, conversion to engineering units is readily accomplished by applying the proper scaling factor. For that matter, the scaling factor need not be linear, such as is required for an output in terms of altitude.

The overall accuracy of the linearized instruments is computed from the statistical sum of a number of errors, each of which is random. Taking into account errors due to damping, repeatability, hysteresis, long term stability, resolution, calibration, linearity, gas density, ambient temperature, and vibration, the total 2σ error for a 20 psia vibrating cylinder pressure transducer with a linear digital output is $\pm$0.012% of full scale. The error for the linear analog instrument is $\pm$0.04% of full scale. We believe that accuracy to this degree in so small and rugged a package is unparalleled.

Many applications could be discussed — they are all interesting, especially because they are all complemented by the subject pressure transducer. Time and space have permitted the discussion of only two of the many interesting uses for digital pressure transducers. The nuclear power plant benefits from the vibrating cylinder pressure transducer because leakage testing of reactor containment is made easier and more accurate. The user likes the idea of not having to recalibrate the instrument every two weeks. The same stability affords the air inlet control the ability to operate for months without drifting off design, a situation which might drastically degrade the performance of supersonic aircraft and put the pilot at a disadvantage when he tries to pursue his assigned mission.

The discussion, analysis, and applications discussed in this paper indicate that the vibrating cylinder digital pressure transducer is an instrument that can be used in the laboratory as well as in the relatively hostile environment found in aircraft systems and process control. Hopefully, with the availability of instruments such as this, the trend toward digital systems will increase, thereby permitting the achievement of accuracy and stability heretofore not available in analog systems. The trend will continue as long as digital instruments can be made simple, reliable, and low in cost.

NOMENCLATURE

A, B, C	= Calibration constants
c	= Damping
$F\{t\}$	= Magnetic forcing function
f	= Frequency
G	= Vibratory amplitude at f_n
H	= Vibratory amplitude at f_1 and f_2
k	= Spring constant of cylinder wall
L	= Inductance of magnetic pickup coil
M.F.	= Magnification factor
m	= Mass
N	= Count
P	= Pressure being measured
Q	= Average energy stored/energy dissipated by damping per cycle
t	= Time
V	= Voltage from magnetic pickup coil
x	= Vibratory amplitude of cylinder wall
$\dot{x}$	= Vibratory velocity of cylinder wall
$\ddot{x}$	= Vibratory acceleration of cylinder wall
ζ	= c/c_c, damping factor
τ	= Period of vibration
ϕ	= Lines of magnetic flux
ψ	= Phase angle between forcing function and vibratory amplitude
ω	= Circular frequency

SUBSCRIPTS

c	= Clock
n	= Natural frequency
o	= Offset pressure or free stream
P	= Pressure measured
S	= Static
T	= Total
t	= Transducer or throat

KEY WORDS

Air Data Computers
Air Data Controls
Digital Sensor
Digital Transducer
Engine Pressure Ratio
Measurements
Pressure
Pressure Measurements
Pressure Sensor
Pressure Transducer
Sensor
Transducer
Vibrating Cylinder

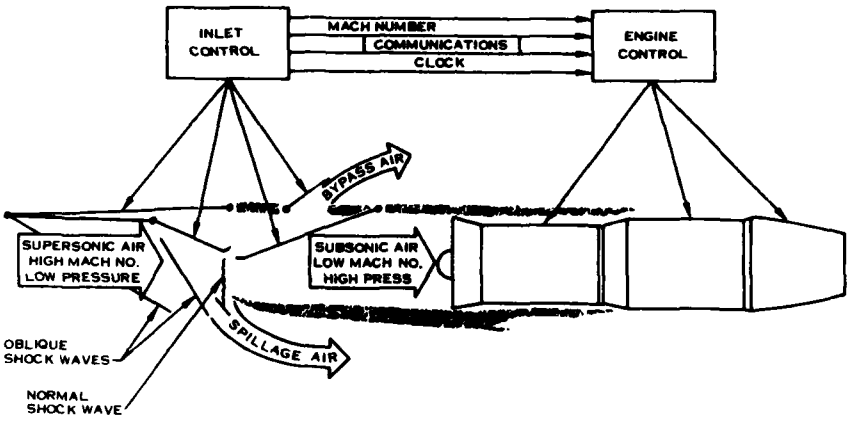

FIGURE 15. SUPERSONIC PROPULSION CONTROL

FIGURE 16. VIEW OF AIR INLET CONTROL PRESSURE TRANSDUCER SUBASSEMBLY

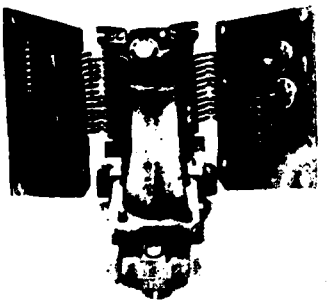

FIGURE 17. VIEW OF VIBRATING CYLINDER PRESSURE TRANSDUCER AND ASSOCIATED ELECTRONICS USED IN AIR INLET CONTROL

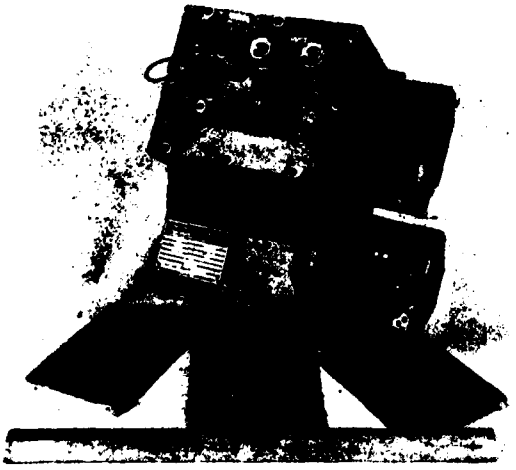

FIGURE 18. AIR INLET CONTROL EXPLODED VIEW

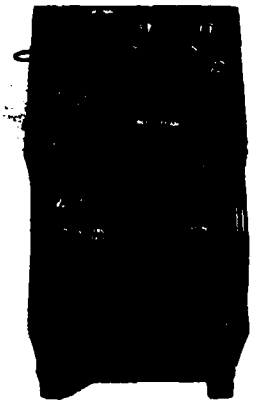

FIGURE 19. AIR INLET CONTROL

APPENDIX II

PRIME ITEM PROCESS SPECIFICATION FOR A LOW COST METHOD OF FABRICATING THIN WALLED CYLINDRICAL SHELLS USING A SPUTTERING PROCESS

Specification Number
Code Identification

September 4, 1980

1.0 SCOPE

1.1 Scope

This specification covers the processing technology used to fabricate thin walled cylindrical shells by sputtering. Thin wall shells can be used as the sensing element in vibrating cylinder pressure transducers.

2.0 APPLICABLE DOCUMENTS

The following documents should be consulted for further background on this process.

United Technologies Research Center Report, R80-924394-8, Final Technical Report - Fabrication of Thin Wall Cylindrical Shells by Sputtering - September 4, 1980.

Thin Film Processes - J. L. Vossen and W. Kern, Academic Press, 1978.

3.0 REQUIREMENTS

3.1 Equipment

The equipment required to perform this process is as follows:

(1) A vacuum chamber, preferably of stainless steel construction, and an associated pumping system which is capable of evacuating the chamber to at least 10^{-6} torr.

(2) Two (2) diode sputtering cathodes and associated impedance matching networks capable of sustaining a minimum power density to the cathode of 50 W/in.^{2}.

(3) Two (2) permanent magnets or two (2) electromagnets capable of producing a quadrupole shaped magnetic field in the vicinity of the targets of maximum local strength of 300 Gauss.

(4) An insulated, rotatable, vacuum feedthrough for 1/2 in. diameter shaft capable of sustaining rotations up to 10 revolutions per minute and being able to hold off at least 500 VDC from electrical ground all the while maintaining a vacuum of at least 10^{-6} torr.

(5) Threaded 1/2 in. diameter hollow 300 series stainless steel shafts for supporting the mandrel substrates fitted with heaters capable of raising the temperature to 650°C and temperature readout.

(6) Two (2) rf sputtering power supplies capable of delivering at least 50 W/in.^{2} of power to the targets.

(7) Pressure gages -- one (1) ionization type to measure system high vacuum and one (1) capacitance monometer type to measure sputtering gas pressure.

(8) Negative dc bias power supplies capable of delivering up to 20 W of power to each mandrel being coated at up to -200 VDC.

(9) One (1) micrometer type valve to regulate sputtering gas flow into the sputtering system.

3.2 Materials

The materials required to perform this process are as follows:

(1) Supply of 99.999% pure Argon sputtering gas
(2) Ni-Span-C Alloy 902 planar sputtering targets
(3) Silicon dioxide sputtering targets
(4) 300 series stainless steel mandrels internally threaded to fit over threaded 1/2 in. diameter hollow shafts.

3.3 Required Procedures and Operations

This paragraph provides the detailed procedures that must be followed to assure that acceptable quality thin wall shells of Ni-Span-C suitable for use as elements in vibrating cylinder pressure transducers are produced by this method.

The targets, the rotating mandrel holder(s), and the magnets are arranged in the sputtering chamber as shown in Fig. II-1. The target-to-mandrel distance is 2.5 in. The third in-line target is added only if it is desired to grow a closed end on the cylindrical shell. In forming simple right circular open-ended shells for pressure transducers, the third target is not required.

Mandrels are prepared for coating by applying a parting layer to them which is compatible with the sputtering process. This parting layer is required so that the sputtered shell can be made to release from the mandrel. A sputtered layer of silicon dioxide approximately 0.5 microns thick on the mandrels provides an excellent parting layer.

Prepared mandrels are threaded onto the rotatable shafts, the sputtering system is closed and evacuated to at least 10^{-6} torr. The mandrel heaters are brought up to 650°C. When the mandrels have reached 650°C, the background gas pressure is brought up to 10^{-2} torr using 99.999% Argon. The mandrels are set rotating and deposition of Ni-Span-C is begun on the mandrels. If the magnetic field is derived from electromagnets, the magnetic field strength is brought up to 300 Gauss before the deposistion is begun. Deposition is carried out with a power density input to the targets of at least 50 W/in.^{2}. After the deposition has proceeded for 15 minutes, a dc bias of -150 V is applied to the mandrels through the rotating shaft. Deposition is then allowed to continue until the proper thickness of material is deposited on the mandrels. With a target-to-mandrel separation of 2.5 in., deposition rate under these conditions will be approximately 5 μm/hr.

After the desired thickness of material has been deposited, the sputtering system is shut down but the system is left under vacuum until the mandrels have cooled to below 100°C. The system is then vented with dry nitrogen gas and the mandrels are allowed to cool to 50°C before removing.

The shells are removed from the mandrels using mechanical methods. First the ends of the mandrel are lightly ground on 400 grit wet emery paper to assure that the shell is not held to the mandrel by the shell extending around the ends of the mandrel. Next, the coated mandrel is lightly cold worked either by burnishing it while having it rotate in a lathe for example, or by lightly glass bead peaning it. A small amount of cold working is sufficient to loosen the shell from the mandrel where it can be easily slid off.

FIG. II-1

PLANAR OPPOSED TARGET SPUTTERING SYSTEM

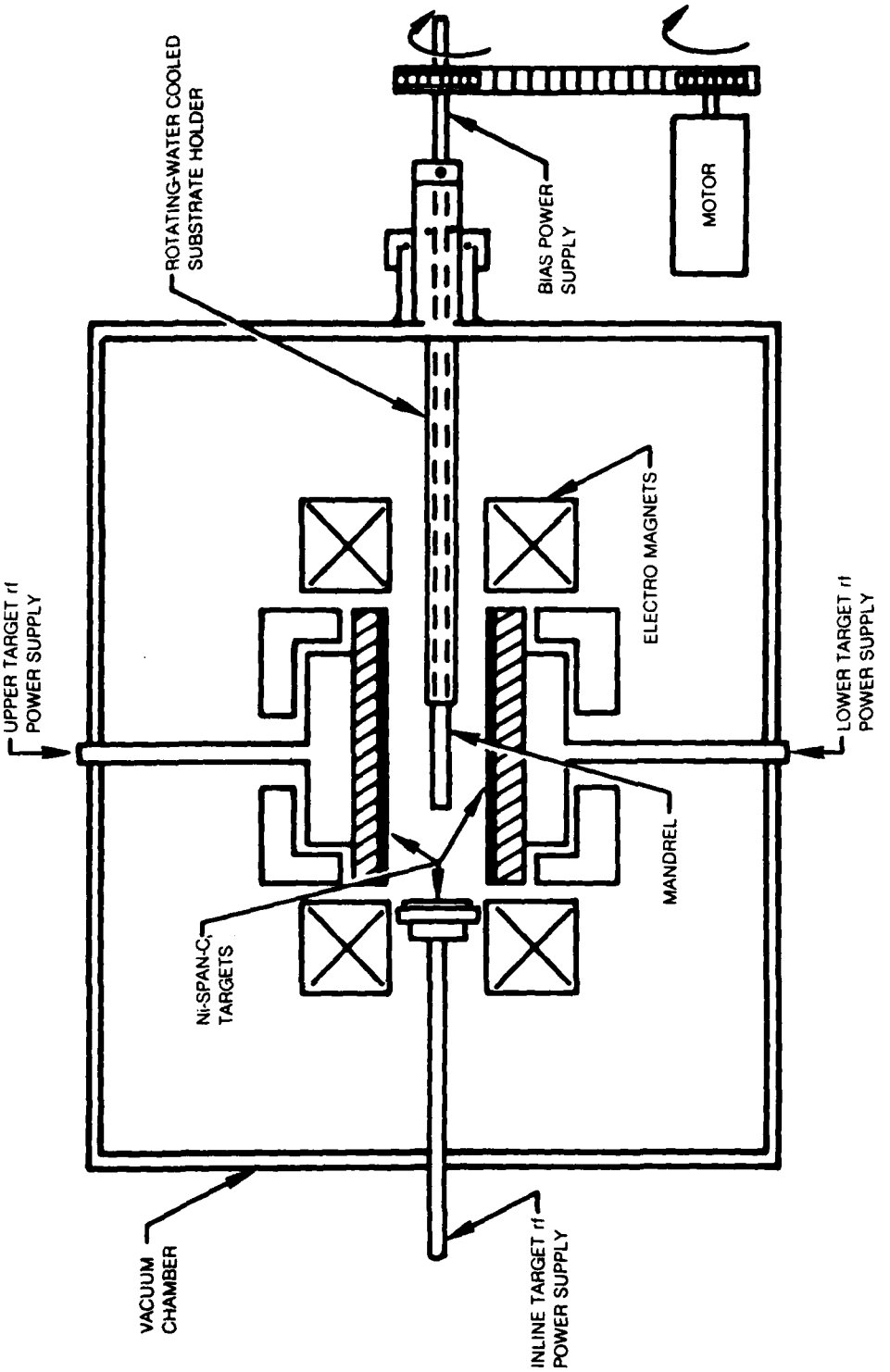

80-8-3-13

4.0 QUALITY ASSURANCE PROVISIONS

The examination and tests to be performed on the deposition equipment must be done by the operator. Before every run the fixturing and shields in the vicinity of the targets and substrates must be cleaned to remove any accumulation of sputtered material from previous deposition runs. Targets must be examined to be sure that the material supply is sufficient for the next planned run. This information can be deduced by measuring and recording the target thickness before every run. In this way target life can be predicted on the basis of run time and deposition parameters. The same kind of inspection and record keeping must be done to assure an adequate sputtering gas supply.

Mandrels to be coated must be free of surface contaminants, especially particulate matter to avoid pin holes in the shell. Before mounting, mandrels are degreased in an inorganic solvent, then washed with detergent in distilled water. Multiple rinses in distilled water followed by drying in a dry nitrogen stream completes the mandrel cleaning process.

A silicon dioxide parting layer approximately 0.5 μm thick is applied to the mandrels by sputtering in essentially the same way that the shell is deposited onto the mandrel. The mandrel is cleaned by degreasing and washing as is done for shell deposition, then it is mounted on a rotating mandrel holder. However, the mandrel need not be heated intentionally, but it can simply be left to rise in temperature due to the sputtering process. The targets must, of course, be silicon dioxide in place of Ni-Span-C. No electrical bias is applied to the mandrels during silicon dioxide coating and power density to the targets should be reduced to 25 $W/in.^2$.

In order to assure that the vacuum system is performing consistently well, a record of the pumping time required to reach a pressure of 10^{-6} torr must be kept. A vacuum of at least this pressure is required before deposition can begin. Any improvement in achieving lower pressures is to be desired and will result in an improved product.

During operation, the sputtering parameters must be kept under close control in order to produce a shell whose mechanical and physical properties are acceptable. Gas pressure, rf power input, dc bias voltage, and mandrel temperature require close control to assure good quality shell fabrication. Because the deposition runs are of such long duration, automatic controllers are much to be desired. Regulation of these deposition parameters must be kept to at least 1 percent.

6.0 NOTES

The intended use of the process described above is for the fabrication of thin wall cylindrical shells as an alternative method to conventional machining. The sputtering method allows a wide variety of materials to be used as the shell material. Some materials such as ceramics for example, could not be machined in the conventional way to form thin wall shells. Specifically, this method was devised to use Ni-Span-C alloy 902 as the source material. This complex alloy is stable, magnetic, and has the special property that its thermoelastic coefficient can be adjusted by heat treating. This alloy has been used for a variety of control applications and in particular, it is the alloy used by Hamilton Standard Division of United Technologies Corporation for the fabrication of a vibrating cylinder pressure transducer. As an illustration of the application of this process, a thin wall vibrating cylinder pressure transducer has been fabricated and operated using a sputtered thin wall cylinder formed using the guide lines of this specification. To be used as the element in the vibrating cylinder pressure transducer, the sputtered thin wall shell had to be fitted with a relatively heavy wall end cap and an equally heavy wall base for mounting. These two heavy wall pieces were machined using conventional techniques from bulk Ni-Span-C. The final configuration was formed by electron beam welding the heavy wall end pieces to the sputtered shell.

Distribution List

Office of the Under Secretary
of Defense, Research and Engineering
(R&AT)
Attn: Dr. Lloyd Lehn
Pentagon
Washington, D.C. 20301

DARPA (MATS)
1400 Wilson Blvd
Arlington, VA 22209

Chief, Office of Manufacturing Technology
U.S. Army Material Development
and Readiness Command
5001 Eisenhower Avenue
Alexandria, VA 22333

Director
Naval Material Command
Industrial Resources Detachment
Bldg.-75-2
Philadelphia, PA 19112

Naval Sea Systems Command
Attn: SEA-05R2
Washington, D.C. 20362

Naval Electronic Systems Command
Attn: ELEX-8134
Washington, D.C. 20360

Air Force Wright Aeronautical Lab
Attn: Manufacturing Technology Division
Wright Patterson AFB
Ohio 45433

Manufacturing Technology
Utilization
NASA Headquarters
600 Independence Ave., SW
Washington, D.C. 20546

Department of Commerce
Director, Office of Cooperative
Generic Technology
Mail Stop 3520
Washington, D.C. 20230

Reliability Analysis Center
Rome Air Development Center
Griffis Air Force Base
Attn: J. L. Krulac RBAC
Rome, NY 13441

Distribution List (cont.)

Defense Documentation Center
Cameron Station, Bldg. 5
Alexandria, VA 22314
Attn: DDC-TC
To Be forwarded Via:
Commander
Naval Air Systems Command
Attn: AIR-0004
Washington, D.C. 20361
(2 copies)

Commander
Naval Air Development Center
Warminster, PA 18974
Attn: Technical Library

Commander
Naval Air Systems Command
Attn: AIR-5143G
Washington, D.C. 20361
(3 copies)

Commanding Officer
Naval Avionics Center
6000 East 21st Street
Indianapolis, IN 46218
Attn: Technical Library

Superintendant
Naval Postgraduate School
Monterey, CA 93940
Attn: Technical Library

Commanding Officer
Naval Research Laboratory
Washington, D.C. 20375
Attn: Technical Library

Sandia Laboratories
P.O. Box 5800
NM 87115
Albuquerque
Attn: Technical Library 3141

United Technologies Research Center
400 Main Street
East Hartford, CT 06108
Attn: Dr. Anthony J. DeMaria

Lawrence Radiation Laboratory
P. O. Box 808
Livermore, CA 94550
Attn: J. W. Dini MS L332

Distribution List (cont.)

Northrop Corp.
Electronics Division
Manufacturing Engr. Unit
2301 W 102th Street
Attn: Donald M. Weaver
Hawthorne, CA 90250

Neil Brown Instrument Systems Inc.
Attn: R. A. Mattey
P.O. Box 498
1140 Route 28A
Cataumet, MA 02534

Transducers, Inc.
14030 Bolsa Lane
Attn: Peter R. Perino
Cerritos, CA 90701

Ametek
Attn: R. A. Russell
Station Square Two
Paoli, PA 19301

Bendix
Aircraft Brake - Strut/
Energy Controls Divisions Library
717 N. Bendix Drive
South Bend, IN 46620

TRW Inc.
401 North Broad Street
Attn: H. B. Casey
Philadelphia, PA 19108

Dressor Industries
Industrial Instrument Operations
Attn: R. Hardcastle
Stratford, Connecticut 06497

TRW Inc.
401 North Broad Street
Attn: Dr. K. M. Merz
Philadelphia, PA 19108


FILMED
8